

GEOMETRICAL PROPERTIES OF THE MEAN-MEDIAN MAP

JONATHAN HOSEANA AND FRANCO VIVALDI

ABSTRACT. We study the mean-median map as a dynamical system on the space of finite sets of piecewise-affine continuous functions with rational coefficients. We determine the structure of the limit function in the neighbourhood of a distinctive family of rational points, the local minima. By constructing a simpler map which represents the dynamics in such neighbourhoods, we extend the results of Cellarosi and Munday [2] by two orders of magnitude. Based on these computations, we conjecture that the Hausdorff dimension of the graph of the limit function of the set $[0, x, 1]$ is greater than 1.

1. INTRODUCTION

Consider a finite multiset¹ $[x_1, \dots, x_n]$ of real numbers. Its *arithmetic mean* and *median* are defined, respectively, as

$$\langle x_1, \dots, x_n \rangle := \frac{1}{n} \sum_{i=1}^n x_i \quad \text{and} \quad \mathcal{M}(x_1, \dots, x_n) := \begin{cases} x_{j_{\frac{n+1}{2}}} & n \text{ odd} \\ \frac{1}{2} (x_{j_{\frac{n}{2}}} + x_{j_{\frac{n}{2}+1}}) & n \text{ even,} \end{cases}$$

where $k \mapsto j_k$ is a permutation of indices $\{1, \dots, n\}$ for which $x_{j_1} \leq x_{j_2} \leq \dots \leq x_{j_n}$.

The set $[x_1, \dots, x_n]$ may be enlarged by adjoining to it a new real number x_{n+1} uniquely determined by the stipulation that the arithmetic mean of the enlarged set be equal to the median of the original set. In symbols:

$$(1) \quad x_{n+1} = (n+1)\mathcal{M}(x_1, \dots, x_n) - n \langle x_1, \dots, x_n \rangle.$$

The map $[x_1, \dots, x_n] \mapsto [x_1, \dots, x_n, x_{n+1}]$ is known as the *mean-median map* (MMM). This map and its iteration was introduced in [11], and subsequently studied in [3, 2, 6]. Such an iteration is meant to generate a set whose mean and median coincide. The order of the recursion grows with the iteration, so that the MMM is a dynamical system over the infinite-dimensional space of all finite sets of real numbers.

The MMM dynamics is novel and intriguing. The evolution of the system depends sensitively on a small cluster of points located around the median, but only on the average—rather than the detailed values—of the rest of the data. From (1) we see that each new element of the set typically results from the difference of two diverging quantities, which is a distinctive source of instability. Finally, the dependence of the median on smooth variations of the data is not smooth, adding complexity.

Since the MMM *preserves affine-equivalences*² [3, section 3], the simplest non-trivial initial sets—those of size three—may be studied in full generality by considering the single-variable

Date: November 11, 2019.

¹Hereafter shall be referred to simply as a *set*. We use square brackets to distinguish it from an ordinary set.

²If $[x_1, \dots, x_n] \mapsto [x_1, \dots, x_n, x_{n+1}]$ then for every $a, b \in \mathbb{R}$ we have $[ax_1 + b, \dots, ax_n + b] \mapsto [ax_1 + b, \dots, ax_n + b, ax_{n+1} + b]$.

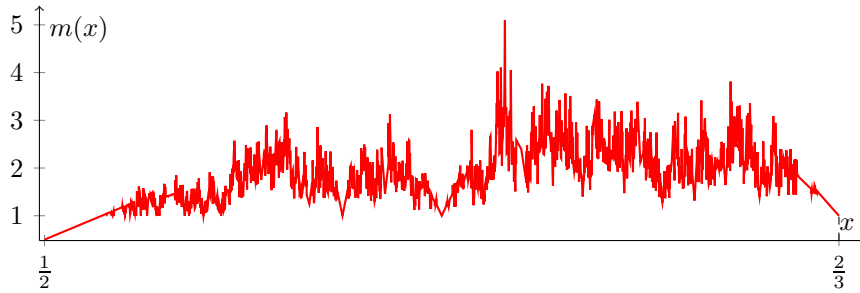


FIGURE 1. A computer-generated image of $m(x)$ for $x \in [\frac{1}{2}, \frac{2}{3}]$. The limit function m may be reconstructed entirely from its values in this interval, due to symmetries. The local minima occur at a prominent set of rational numbers.

initial set $[0, x, 1]$, with $x \in [0, 1]$ referred to as the *initial condition*. Here one finds already substantial difficulties, which are synthesised in the following conjectures [11, 3].

Conjecture 1 (Strong terminating conjecture). *For every $x \in [0, 1]$ there is an integer τ such that $x_{\tau+k} = x_\tau$ for all $k \in \mathbb{N}$.*

Such an integer τ , if it exists, will be assumed to be minimal, thereby defining a real function $x \mapsto \tau(x)$, called the *transit time*. At values of $x \in [0, 1]$ for which such an integer does not exist, we set $\tau(x) = \infty$. If the *orbit* $(x_n)_{n=1}^\infty$ converges at x —with finite or infinite transit time—then we have a real function $x \mapsto m(x)$, called the *limit function*, which gives the limit of this sequence as a function of the initial condition. This function has an intricate, distinctive structure, shown in figure 1. Moreover, since the *median sequence* $(\mathcal{M}_n)_{n=3}^\infty$, where $\mathcal{M}_n := \mathcal{M}(x_1, \dots, x_n)$, is monotonic [3, theorem 2.1], writing

$$\begin{aligned}
 m &= \lim_{N \rightarrow \infty} \mathcal{M}_N \\
 &= \lim_{N \rightarrow \infty} \left[\mathcal{M}_3 + \sum_{n=4}^N (\mathcal{M}_n - \mathcal{M}_{n-1}) \right] \\
 (2) \quad &= \mathcal{M}_3 + \sum_{n=4}^{\infty} (\mathcal{M}_n - \mathcal{M}_{n-1}),
 \end{aligned}$$

we see that, in a domain of monotonicity, the limit function is the sum of non-negative (say) piecewise-affine continuous functions with finitely many singularities³.

Conjecture 2 (Continuity conjecture). *The function $x \mapsto m(x)$ is continuous.*

In [3], both conjectures were proved to hold within an explicitly-determined real neighbourhood of $x = \frac{1}{2}$, where m turns out to be affine. Using a computer-assisted proof, this result was then substantially extended in [2], where the limit function was constructed in neighbourhoods of all rational numbers with denominator at most 18 lying in the interval $[\frac{1}{2}, \frac{2}{3}]$. The measure of these neighbourhoods adds up to only 11.75% of the measure of the interval. The authors also identified 17 rational numbers at which m is non-differentiable. In [6], a long initial segment of the MMM sequence was computed for $x = \frac{\sqrt{5}-1}{2}$, and, up to

³In this paper, a singularity means a point of non-differentiability.

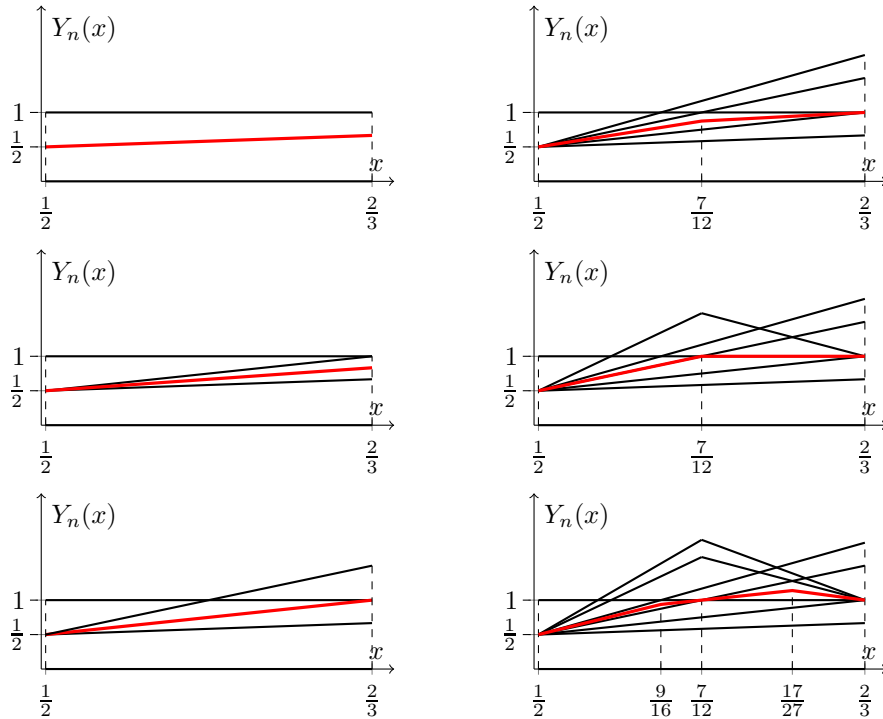


FIGURE 2. Early evolution of the bundle $[0, x, 1]$. In each picture, the red function is the current median.

stabilisation, for some convergents of the continued fraction expansion of x , using exact arithmetic in $\mathbb{Q}(\sqrt{5})$ and \mathbb{Q} , respectively. The results suggest that τ becomes unbounded along the sequence of convergents, that is, the transit time at x could be infinite. Thus, although the strong terminating conjecture seems to hold over \mathbb{Q} , it may fail in larger fields.

Motivated by these studies of the system $[0, x, 1]$, we introduce the *functional* MMM which acts on the space of finite sets of piecewise-affine continuous functions with rational coefficients; we refer to such sets as *bundles*⁴. Observing the early evolution of the bundle $[0, x, 1]$ (figure 2), we can see that a local minimum of the limit function (figure 1) first appears as a transversal intersection of bundle elements; we refer to such a point as an *X-point*. The aim of this paper is to present a theory of the dynamics of the MMM in the vicinity of X-points.

We now describe the organisation and main results of this paper. In section 2 we introduce the preliminary concepts: cores, bundles, and X-points, including *bundle equivalence* which generalises affine-equivalence of two real sets. In section 3 we show that for any two functions forming an X-point and an auxiliary function —any function not through the X-point— there is a local symmetry which induces a self-equivalence of the subbundle containing these three functions. The symmetry is a homology (theorem 4) which is harmonic in a significant special case (corollary 5), except at X-points where the median sequence reverses its monotonicity (theorem 6).

In section 4 we prove that the strong terminating conjecture holds globally for the bundle $[0, x, 1, 1]$ (theorem 9) using a method which minimises computer assistance.

⁴This is unrelated to the standard notion of *fibre bundles* in topology.

In section 5 we develop conditions for which the symmetry of an X-point becomes a symmetry of the limit function (lemmas 10 and 11, theorem 13). Then we use our knowledge of the dynamics of $[0, x, 1, 1]$ to establish the local structure of the limit function near general X-points (theorems 14 and 16). Of note is the existence of a hierarchy of X-points, whereby an X-point typically generates an *auxiliary sequence* (theorem 15) of like points. Auxiliary sequences form the scaffolding of the intricate structure of local minima of the limit function seen in figure 1. Subsequently, we justify the assumptions of our main theorems by illustrating various pathologies.

In section 6 we introduce the *normal form* of the MMM, a one-parameter family of dynamical systems over \mathbb{Q} which, after a suitable rescaling, represent the dynamics near any X-point with a given transit time (proposition 17). This simplification results from the fact that the local dynamics is largely unaffected by its earlier history. We show that a normal form orbit has a regular initial phase (lemma 18), which we then exploit to derive lower bounds for the limit and the transit time (theorem 19). We also show that during this phase, the iterates have low arithmetic complexity⁵ (corollary 20).

In the last section, we describe the results of exact computations on the system $[0, x, 1]$, made possible by the theory just developed. We have established the strong terminating conjecture in specified neighbourhoods of 2791 rational numbers in the interval $[\frac{1}{2}, \frac{2}{3}]$, thereby extending the results of [2] by two orders of magnitude. This large data collection makes it clear that the domains over which the limit function is regular do not account for the whole Lebesgue measure, suggesting the existence of a drastically different, yet unknown, dynamical behaviour. For a quantitative assessment of this phenomenon, we have computed the variation of the limit function with respect to Farey fractions, and with respect to dyadic fractions. In both cases, the variation is observed to grow algebraically with the size of the partition, with comparable exponents, suggesting the following conjecture.

Conjecture 3. *The Hausdorff dimension of the graph of the limit function of the system $[0, x, 1]$ is greater than 1.*

The representation (2) of the limit function (a sum of piecewise-affine saw-tooth functions of irregularly decreasing amplitude) makes unbounded variation plausible (as with Takagi-type functions [1, 7]). However, the nature of the conjectured domains of unbounded variation is far more elusive, and is clearly relevant to the continuity conjecture. This problem deserves further investigation.

2. PRELIMINARIES

We first define the *core* of a real set and use it to write an alternative formula for MMM recursion which will be useful later. Then we define our two main objects of study: *bundles* and *X-points*.

2.1. Cores. The *core* of a real set $\xi = [x'_1, \dots, x'_n]$, $n \geq 2$, whose elements are written in non-decreasing order, i.e., $x'_1 \leq \dots \leq x'_n$, is the subset containing its two (three, respectively)

⁵In our understanding, the ubiquity of stabilising sequences over \mathbb{Q} is closely related to the slow growth of the arithmetic complexity of their terms.

central elements if n is even (odd, respectively), i.e.,

$$(3) \quad \lambda := \begin{cases} \left[\frac{x'_n}{2}, \frac{x'_{n+1}}{2} \right] & \text{if } n \text{ is even} \\ \left[\frac{x'_{n-1}}{2}, \frac{x'_{n+1}}{2}, \frac{x'_{n+3}}{2} \right] & \text{otherwise.} \end{cases}$$

The core is said to be *odd* if n is odd, and *even* if n is even. In the context of ξ being an iterate, i.e., when it is written as ξ_n , where $n = |\xi|$, we may denote its core by λ_n .

Let ξ be an initial set for which the median sequence is non-decreasing. We prove two lemmas which clarify the importance of cores.

Lemma 1. *Let $n \geq |\xi| + 2$ be odd, and let $i \in \{1, \dots, n-2\}$, $j \in \{1, \dots, n-1\}$ such that $\mathcal{M}_{n-1} = \langle x_i, x_j \rangle$ and $\mathcal{M}_{n-2} = x_i$. Then $x_n \geq x_j$ with equality if and only if $x_i = x_j$.*

Proof. Let $n \geq |\xi| + 2$ be odd. Notice that

$$x_n = n\mathcal{M}_{n-1} - (n-1)\mathcal{M}_{n-2} = n\langle x_i, x_j \rangle - (n-1)x_i = \left(\frac{n}{2} - 1\right)(x_j - x_i) + x_j \geq x_j,$$

proving the lemma. \square

Lemma 2. *Let $n \geq |\xi| + 3$ be an integer.*

i) *If n is even, then there exist $i \in \{1, \dots, n-3\}$ and $j \in \{1, \dots, n-2\}$ such that $\mathcal{M}_{n-3} = x_i$, $\mathcal{M}_{n-2} = \langle x_i, x_j \rangle$, $\mathcal{M}_{n-1} = x_j$. Moreover,*

$$(4) \quad x_n - x_{n-1} = \mathcal{M}_{n-1} - \mathcal{M}_{n-3},$$

and $x_n \geq x_{n-1} \geq x_j \geq x_i$ with equality if and only if $x_i = x_j$.

ii) *If n is odd, then there exist $i, j \in \{1, \dots, n-3\}$ and $k \in \{1, \dots, n-1\}$ such that $\mathcal{M}_{n-3} = \langle x_i, x_j \rangle$, $\mathcal{M}_{n-2} = x_j$, $\mathcal{M}_{n-1} = \langle x_j, x_k \rangle$. Moreover,*

$$(5) \quad x_n - x_{n-1} = \frac{n}{2}(x_k - x_j) - \frac{n-2}{2}(x_j - x_i),$$

and $x_n < x_{n-1}$ if and only if

$$(6) \quad \frac{x_k - x_j}{x_j - x_i} < 1 - \frac{2}{n}.$$

Proof. Let $n \geq |\xi| + 3$. First suppose n is even. Then there are indices $i \in \{1, \dots, n-3\}$ and $j \in \{1, \dots, n-2\}$ for which $\mathcal{M}_{n-3} = x_i$, $\mathcal{M}_{n-2} = \langle x_i, x_j \rangle$, and $\mathcal{M}_{n-1} = x_j$. Notice that lemma 1 guarantees that the median \mathcal{M}_{n-1} must be the larger element of which the previous median \mathcal{M}_{n-2} is the average; we can not have $\mathcal{M}_{n-1} = x_{n-1} < x_j$. Moreover, we have

$$(7) \quad x_n = n\mathcal{M}_{n-1} - (n-1)\mathcal{M}_{n-2} \quad \text{and} \quad x_{n-1} = (n-1)\mathcal{M}_{n-2} - (n-2)\mathcal{M}_{n-3}.$$

After substituting the above median expressions, subtracting these two equations gives (4). Moreover, the second equation in (7) is equivalent to

$$x_{n-1} - x_j = \frac{n-3}{2}(x_j - x_i).$$

Since $x_j \geq x_i$, then the last equation implies $x_{n-1} \geq x_j$, whereas the second-to-last implies $x_n \geq x_{n-1}$, and hence $x_n \geq x_{n-1} \geq x_j \geq x_i$. If $x_i = x_j$, then the second-to-last equation gives $x_n = x_{n-1}$, whereas the last one implies $x_n = x_j$, meaning that these numbers are all equal.

Now suppose n is odd. Then there are indices $i, j \in \{1, \dots, n-3\}$ and $k \in \{1, \dots, n-1\}$ for which $\mathcal{M}_{n-3} = \langle x_i, x_j \rangle$, $\mathcal{M}_{n-2} = x_j$, and $\mathcal{M}_{n-1} = \langle x_j, x_k \rangle$, where, once again, lemma 1

forbids the case $\mathcal{M}_{n-2} = x_{n-2} < x_j$. Substituting these median expressions to (7) gives (5). Notice that $x_n < x_{n-1}$ if and only if its right-hand side is negative. \square

Thus, for every $n \geq |\xi| + 2$, the MMM recursion (1) can be written in terms of the elements of the core λ_{n-2} :

$$(8) \quad x_n = \begin{cases} x_{n-1} + (x_j - x_i) & n \text{ even, } \lambda_{n-2} = [x_i, x_j] \\ x_{n-1} + \frac{n}{2}(x_k - x_j) - \frac{n-2}{2}(x_j - x_i) & n \text{ odd, } \lambda_{n-2} = [x_i, x_j, x_k], \end{cases}$$

where the core elements are written in non-decreasing order.

2.2. Bundles and X-points. A *bundle* is a finite (multi)set of univariate piecewise-affine continuous real functions having rational coefficients and finitely many pieces on any interval. A bundle is *regular* if all its elements are affine. A subset of a bundle is called a *subbundle*.

The arithmetic mean $\langle \Xi \rangle$ and median $\mathcal{M}(\Xi)$ of a bundle $\Xi = [Y_1, \dots, Y_n]$ are defined pointwise, i.e.,

$$\langle \Xi \rangle(x) := \langle \Xi(x) \rangle \quad \text{and} \quad \mathcal{M}(\Xi)(x) := \mathcal{M}(\Xi(x)),$$

where $\Xi(x) := [Y_1(x), \dots, Y_n(x)]$, for every $x \in \mathbb{R}$. One verifies that these are also piecewise-affine continuous real functions with rational coefficients, and hence so is [cf. (1)]

$$(9) \quad \mathbf{M}(\Xi) := |\Xi|(\mathcal{M}(\Xi) - \langle \Xi \rangle) + \mathcal{M}(\Xi).$$

Consequently, we can define the *functional* MMM \mathbf{M} as a self-map on the space of all bundles via

$$(10) \quad \mathbf{M}(\Xi) := \Xi \uplus [\mathbf{M}(\Xi)],$$

where the set union operator increases the multiplicity of the function $\mathbf{M}(\Xi)$ in Ξ by 1 to obtain $\mathbf{M}(\Xi)$.

Furthermore, any subfield \mathbb{L} of \mathbb{R} is invariant under all bundle functions as well as their MMM images (9), so it is possible to consider the restricted setting $Y_i : \mathbb{L} \rightarrow \mathbb{L}$. It then makes sense to begin the study of bundle dynamics from the case $\mathbb{L} = \mathbb{Q}$, that is, to consider the restriction of bundles to rational points.

Given an initial bundle $\Xi_{n_0} = [Y_1, \dots, Y_{n_0}]$, iterating the MMM produces a recursive sequence of bundles $(\Xi_n)_{n=n_0}^\infty$ and a functional orbit $(Y_n)_{n=1}^\infty$ given by

$$\Xi_{n+1} = \Xi_n \uplus [Y_{n+1}], \quad \text{where} \quad Y_{n+1} = \mathbf{M}(\Xi_n), \quad \text{for every } n \geq n_0,$$

together with the associated median sequence $(\mathcal{M}_n)_{n=n_0}^\infty$, where $\mathcal{M}_n := \mathcal{M}(\Xi_n)$, bearing in mind that this is no longer a sequence of numbers, but a sequence of functions which is piecewise monotonic by

$$(11) \quad Y_{n+1} = n(\mathcal{M}_n - \mathcal{M}_{n-1}) + \mathcal{M}_n, \quad \text{for every } n \geq n_0 + 1.$$

The transit time τ and the limit m as functions of the initial bundle, if they exist, are defined pointwise. To emphasise the dependence of the MMM dynamics on the initial bundle, we also call an initial bundle a *system*.

From (11) it also follows that the functional orbit stabilises if and only if the median sequence stabilises [3, theorem 2.3]. At points where this holds, the sum (2) is finite. While *local* stabilisation—which holds in an open interval—has been established near some rational points in the works mentioned earlier [11, 2], global stabilisation is a much stronger property.

Let Ξ and Ξ' be two bundles of the same size. If there is a Möbius transformation μ with rational coefficients and an affine transformation f with coefficients in $\mathbb{Q}(x)$ such that for all $x \in \mathbb{R}$ we have

$$(12) \quad f(\Xi'(x)) = \Xi(\mu(x)),$$

where f acts on a set elementwise without cancellations, then we say that Ξ and Ξ' are *equivalent*, written $\Xi \sim \Xi'$, *via the pair* (μ, f) . Bundle equivalence is a generalisation of affine-equivalence of real sets.

The *upper* and *lower concatenations* of two bundle functions Y and Y' are

$$Y \vee Y' := \max \{Y, Y'\} \quad \text{and} \quad Y \wedge Y' := \min \{Y, Y'\},$$

respectively, where the maximum and minimum are defined pointwise. Notice that $[Y, Y'] \sim [Y \wedge Y', Y \vee Y']$, showing that $\Xi \sim \Xi'$ with μ and f being the identity function does not imply $\Xi = \Xi'$.

By (10) and the commutation relations

$$\mathcal{M}(f(\Xi(x))) = f(\mathcal{M}(\Xi)(x)) \quad \text{and} \quad \langle f(\Xi(x)) \rangle = f(\langle \Xi(x) \rangle)$$

valid for any bundle Ξ and any $x \in \mathbb{R}$, we have

$$f(\mathbf{M}(\Xi)(x)) = \mathbf{M}(f(\Xi(x))).$$

Thus, if $\Xi \sim \Xi'$ then

$$f(\mathbf{M}(\Xi')(x)) = \mathbf{M}(\Xi)(\mu(x)),$$

i.e., $\mathbf{M}(\Xi) \sim \mathbf{M}(\Xi')$, from which it follows inductively that $\mathbf{M}^n(\Xi) \sim \mathbf{M}^n(\Xi')$ for every $n \geq \mathbb{N}_0$. In other words, the functional MMM *preserves bundle equivalences*. We shall also say that a bundle equivalence is *inherited* through the MMM dynamics.

Most bundle equivalences discussed in this paper are non-trivial local *self-equivalences* $\Xi \sim \Xi$. Since these are inherited by the orbit of Ξ , they result in a local functional equation for the limit function m :

$$(13) \quad f(m(x)) = m(\mu(x)).$$

In section 5, we shall see that it is possible to achieve (13) only by establishing a self-equivalence $\Omega \sim \Omega$ of an appropriately chosen subbundle $\Omega \subseteq \Xi$, rather than that of the whole bundle.

The phase space of the MMM is very large, and not all initial bundles deserve attention. To minimise redundancies, initial bundles Ξ are to be chosen to satisfy the following properties:

- i) Ξ is not the image under \mathbf{M} of another bundle, except at isolated points;
- ii) the regions where $\mathcal{M}(\Xi) = \langle \Xi \rangle$ are isolated points;
- iii) not all lines in Ξ are concurrent (including points at infinity).

Condition ii) prevents immediate stabilisation on a positive-measure subdomain, while iii) excludes bundles which are equivalent to a rational set.

For example, the initial bundles $[0, x, 1]$ and $[0, x, 1, 1]$ satisfy these conditions. The median sequence of the latter bundle is globally non-decreasing. By contrast, for the former bundle, the real line may be subdivided into regions where the median sequence is non-increasing and non-decreasing, separated by isolated points [from ii)] where the mean of the bundle is equal to its median. Since these two regions are connected by a self-equivalence of the bundle [3, theorem 3.1], there is no need to study these two regions separately. In the rest of this paper we shall therefore assume that the median sequence is locally non-decreasing. We shall deal

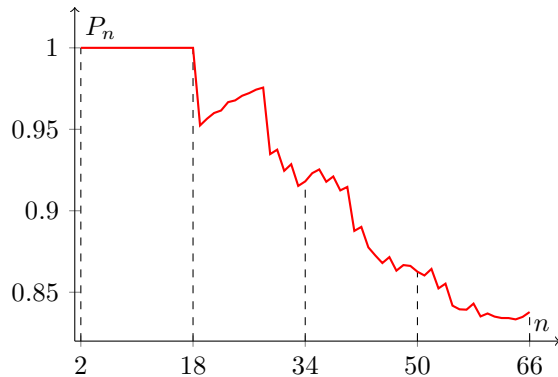


FIGURE 3. The decay of the proportion P_n of fractions with denominator at most n in the interval $[\frac{1}{2}, \frac{2}{3}]$ which are X-points.

separately with the points at which the median sequence reverses its monotonicity (theorem 6 in section 3).

If two functions Y_i and Y_j intersect *transversally* at $p \in \mathbb{Q}$, meaning that there exists $\epsilon > 0$ such that

$$(p - \epsilon, p + \epsilon) \cap \{x \in \mathbb{Q} : Y_i(x) = Y_j(x)\} = \{p\},$$

then we write $p = Y_i \bowtie Y_j$ and refer to p as an *X-point*⁶ (figure 4). Notice that this definition also includes a transversal intersection of more than two functions, say Y_i , Y_j , and Y_k ; such a point is also an X-point which can be written using any pair of subscripts. In a geometrical context, the term X-point and the same notation shall also be used to mean the actual point on the plane rather than its abscissa. An X-point $p = Y_i \bowtie Y_j$ is *regular* if both Y_i and Y_j are regular at p , and is *singular* otherwise.

In the system $[0, x, 1]$, most low-complexity rationals in $[\frac{1}{2}, \frac{2}{3}]$ are X-points; the proportion decreases as complexity increases. This is shown in figure 3, where it is also seen that the smallest denominator of any rational in that interval which is not an X-point is 19. It is therefore fitting that the authors of [2] restricted their computations to rational numbers with denominator at most 18. In their algorithm, X-points appear as the endpoints of intervals where the combinatorics of the MMM orbits remains the same.

X-points are the source of singularities. Indeed, if a bundle Ξ_n is regular then its image bundle Ξ_{n+1} is singular at $p \in \mathbb{Q}$ if and only if the median \mathcal{M}_n is singular at p , in which case p is an X-point incident with \mathcal{M}_n or with one of the functions of which \mathcal{M}_n is the average (see figure 4). Figure 2 illustrates how such singularities develop gradually in the system $[0, x, 1]$ to become as ubiquitous as seen in figure 1.

Let us introduce some terminology concerning X-points. An X-point is *monotonic* if it has a neighbourhood where the median sequence is either non-decreasing or non-increasing. A monotonic X-point p appearing above (below, respectively) the current median in the former (latter, respectively) case guarantees the existence of $m(p)$ by [3, theorem 2.4]. For this reason, the limit function of the system $[0, x, 1]$ exists at every X-point in $[\frac{1}{2}, \frac{2}{3}]$. There are X-points, such as $\frac{1}{2}$ for the bundle $[0, x, 1]$, at which the increments of the median change sign; these are not monotonic.

⁶This definition is local, so $Y_i \bowtie Y_j$ denotes a point rather than a set of points.

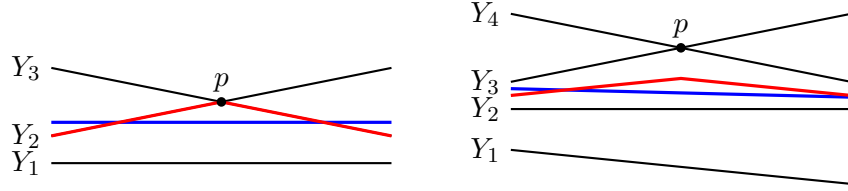


FIGURE 4. Origin of a singularity in a regular bundle Ξ_n , if n is odd ($n = 3$, left) and if n is even ($n = 4$, right). The blue and red functions are the mean and median of the bundle, respectively. The latter is singular, due to the presence of the X-point p . In either case, the image function Y_{n+1} will be singular at p .

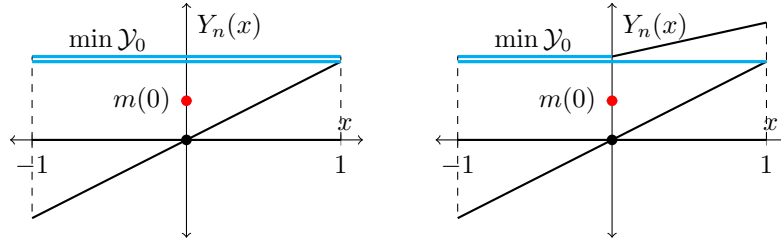


FIGURE 5. The bundle $[0, x, 1, 1]$ in which the origin is an X-point of rank 2 (left) and the bundle $[0, x, 1, Y_4(x)]$, where $Y_4(x)$ is equal to 1 for $x \leq 0$ and to $\frac{x}{2} + 1$ for $x > 0$, in which it is an X-point of left-rank 2 and right-rank 1.

An X-point p *stabilises* (or is *stabilising*) if $\tau(p) < \infty$. A stabilising X-point $p = Y_i \bowtie Y_j$ is *proper* if $\{Y_i, Y_j\}$ is the only pair of functions in the bundle $\Xi_{\tau(p)-1}$ which intersect transversally at the point $(p, Y_i(p))$ and Y_i, Y_j both have multiplicity 1 in the same bundle. If the median sequence is non-decreasing, we associate to every stabilising monotonic X-point $p = Y_i \bowtie Y_j$ in the bundle $\Xi_{\tau(p)-1}$ the set⁷

$$(14) \quad \mathcal{Y}_p := \{Y \in \Xi_{\tau(p)-1} : \Xi_{\tau(p)-1}(p) \cap (Y_i(p), Y(p)) = \emptyset, m(p) \in [Y_i(p), Y(p)]\}.$$

If $\mathcal{Y}_p \neq \emptyset$, then we say that the stabilising X-point p is *active*⁸, and as we shall see in section 5, the function $\min \mathcal{Y}_p$ will be of particular importance. On the left-hand side of p , the multiplicity of this function in the bundle $\Xi_{\tau(p)-1}$ is said to be the *left-rank* of p . Similarly we define the *right-rank* of p in its right-hand side. If these two numbers are equal, then the common value is said to be the *rank* of p . In the system $[0, x, 1]$, every rational number in $[\frac{1}{2}, \frac{2}{3}]$ with denominator between 3 and 18 inclusive studied in [2] is an X-point which is regular, monotonic, proper, active, and of rank 1. Two examples of X-points which are not of rank 1 are presented in figure 5.

A regular stabilising X-point formed by functions whose multiplicities in the bundle $\Xi_{\tau(p)-1}$ are not all 1 has a simpler dynamics, which we shall now present. At such an X-point the limit function is regular but the transit time function has a jump discontinuity. To lighten up the notation, we write inequalities of functions ($Y_i > Y_j$ or $Y_i > c$, with c a constant), to

⁷In its proper meaning, i.e., ignoring multiplicities.

⁸In such a case, we usually have $|\mathcal{Y}_p| = 1$, but this is not always the case. For instance, $\frac{13}{23} = Y_7 \bowtie Y_9$ is an X-point in the system $[0, x, 1]$ for which we have $\mathcal{Y}_{\frac{13}{23}} = \{Y_{10}, Y_{19}\}$.

denote pointwise inequalities ($Y_i(x) > Y_j(x)$ or $Y_i(x) > c$), valid for all points in the domain under consideration.

Lemma 3. *Let $p = Y_i \bowtie Y_j$ be a regular stabilising X-point with $Y_i < Y_j$ if $x > p$, where the multiplicities of Y_i and Y_j in $\Xi_{\tau(p)-1}$ are 1 and at least 2, respectively. Also assume that, locally,*

$$(15) \quad \mathcal{M}_n = Y_i \wedge Y_j \quad \text{and} \quad \mathcal{M}_{n+1}(x) = \begin{cases} Y_j(x) & \text{if } x < p \\ \langle Y_i, Y_j \rangle(x) & \text{if } x \geq p, \end{cases}$$

for an odd integer n . Then near p we have $m(x) = Y_j(x)$ and

$$(16) \quad \tau(x) = \begin{cases} n+2 & \text{if } x < p \\ n+4 & \text{if } x \geq p. \end{cases}$$

Proof. If $x < p$, then (11) easily gives $Y_{n+2} = Y_j$, and hence $m(x) = Y_j(x)$ and $\tau(x) = n+2$. If $x \geq p$, we use (11) to compute Y_{n+2} , Y_{n+3} , and Y_{n+4} . Firstly, $Y_{n+2} = \frac{n}{2}(Y_j - Y_i) + Y_j$, which lies above Y_j since $Y_j > Y_i$. Next, since the median sequence is non-decreasing, then $\mathcal{M}_{n+3} = \mathcal{M}_{n+2} = Y_j$, and so we obtain $Y_{n+3} = \frac{n+2}{2}(Y_j - Y_i) + Y_j$, which also lies above Y_j . Finally, $Y_{n+4} = Y_j$, and hence $m(x) = Y_j(x)$ and $\tau(x) = n+4$, completing the proof. \square

In lemma 3, the limit function is regular but the transit time increases by 2. If instead we assume that $Y_i < Y_j$ if $x < p$, and we modify accordingly equation (15), we obtain a mirror version of (16) describing a *decrease* by 2 of the transit time.

3. SYMMETRIES

This section is devoted to the discussion of geometrical aspects of a bundle, without regard for the dynamics. Specifically, we describe two-dimensional projective collineations determined by an X-point $p = Y_i \bowtie Y_j$ and an *auxiliary function* Y , which is any piecewise-affine function not through p , assuming that all these functions are locally regular except, possibly, at p .

The subbundle containing only these three functions will be called a *triad* and denoted by $\Omega = [Y_i, Y_j; Y]$. The projective collineation induces a non-trivial self-equivalence $\Omega \sim \Omega$, i.e.,

$$(17) \quad f(\Omega(x)) = \Omega(\mu(x)),$$

which holds for all x sufficiently close to p and is specified by a pair of Möbius and affine transformations (μ, f) . Later in section 5, we shall develop suitable conditions under which such a symmetry is inherited by the limit function [cf. (13)], i.e., under which (17) implies (13) for all x sufficiently close to p , for the same pair (μ, f) .

We shall use some concepts of projective geometry (for background, see [4]). We identify the point $(x, y) \in \mathbb{Q}^2$ with the projective point $(x, y, 1) \in \mathbb{P}^2(\mathbb{Q})$, represented with homogeneous coordinates, and we denote by $o_\infty := (0, 1, 0)$ the point at infinity on the ordinate axis [the line $(1, 0, 0)$]. The symbol Y shall be used to denote both a function and its graph. If Y is locally regular, by the *line* Y we mean the graph of the affine extension of Y .

Typically, the symmetry of a triad will be a *homology*, namely a projective collineation with a line of fixed points (the axis) and an additional fixed point (the centre) not on the axis (theorem 4). This type of symmetry will be useful for X-points which are monotonic. If the X-point is also regular, then the homology is *harmonic*, and hence the associated Möbius

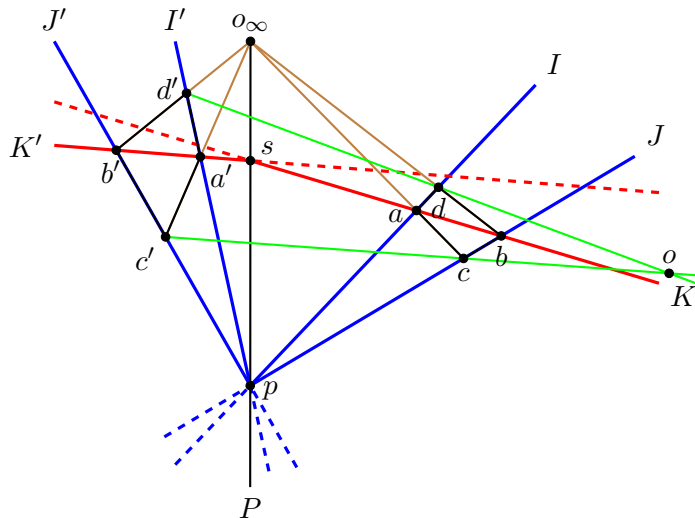


FIGURE 6. Construction of the homology λ determined by the triad $[U, L; Y]$. Here $U = I \vee I'$ and $L = J \vee J'$.

transformation μ is involutory (corollary 5). The second type of symmetry is a more general projectivity which is needed to handle non-monotonic X-points (theorem 6).

3.1. Symmetry of triads. We shall construct a ratio-preserving symmetry for a triad $\Omega = [Y_i, Y_j; Y]$. After defining the concatenations

$$U := Y_i \vee Y_j \quad \text{and} \quad L := Y_i \wedge Y_j,$$

we have $[Y_i, Y_j; Y] \sim [U, L; Y]$, and we shall use the latter triad for our analysis. We introduce the regular functions I, J, K, I', J', K' as follows:

$$(18) \quad \Omega(x) = [U, L; Y](x) = \begin{cases} [I, J; K](x) & \text{if } x \geq p \\ [I', J'; K'](x) & \text{if } x < p. \end{cases}$$

On the affine plane, we have $J < I < K$ for $x > p$ and $J' < I' < K'$ for $x < p$. The symmetry is described by the following theorem.

Theorem 4. *The triad Ω given by (18) determines a homology λ , with axis po_∞ which maps I, J, K to I', J', K' , respectively. This homology induces a self-equivalence of Ω via the pair (μ, f) given by*

$$(19) \quad \mu = \left(\frac{K' - I'}{K' - J'} \right)^{-1} \circ \frac{K - I}{K - J}$$

and

$$(20) \quad f(z) = \frac{K'(\mu(x)) - I'(\mu(x))}{K(x) - I(x)} z + \frac{K(x) \cdot I'(\mu(x)) - I(x) \cdot K'(\mu(x))}{K(x) - I(x)}.$$

This self-equivalence is unique up to inversion. The inverse of μ and the corresponding f are obtained by interchanging all primed and unprimed quantities.

Proof. With reference to figure 6, we let U be a concatenation of I and I' , L a concatenation of J and J' , and Y a concatenation of K and K' , with the stipulation that primed (unprimed) quantities represent the functions to the left (right) of the X-point. We consider the projective collineation λ determined by the following data:

$$(21) \quad \lambda(I) = I', \quad \lambda(J) = J', \quad \lambda(K) = K', \quad \lambda(o_\infty) = o_\infty.$$

From (18) and the remark following it, λ is not the identity. We have $\lambda(p) = I' \cdot J' = p$, and hence the line $P := po_\infty$ is invariant. The point $s := P \cdot K$ is also invariant, as $\lambda(s) = P \cdot K' = s$, and hence λ fixes P pointwise. Since p, s, o_∞ are distinct, the points

$$a := I \cdot K, \quad b := J \cdot K, \quad c := J \cdot (o_\infty a), \quad d := I \cdot (o_\infty b)$$

are vertices of a quadrangle with no vertex on P . The map λ sends this quadrangle to its image $a'b'c'd'$, which is also a quadrangle, as λ preserves incidence. Since λ is not the identity, it can fix at most one of these vertices. If such a fixed vertex exists, then we call it o , and λ is a homology with axis P and centre o .

If there is no fixed vertex, then we define the following lines:

$$(22) \quad A := aa', \quad B := bb', \quad C := cc', \quad D := dd'.$$

All these lines are invariant under λ since their intersection with P is a fixed point, and none of these lines coincides with P . Furthermore, no three of them can coincide; indeed if $A = B = C$, say, then a, b, c would be collinear. Thus least two of these lines must be distinct, and we claim that they must be concurrent at a point, which we shall call o . Indeed if two lines meet at o , a third line not passing through o would result in two (if o is on P) or three (if o is not on P) fixed points of λ lying outside P , making λ the identity.

If o and P were incident, then, on the affine plane one would have J' lying above I' on the left of p , as easily verified, contradicting (18). Thus o and P are not incident, and λ is a homology.

Let us now consider the action of λ on lines through o_∞ . Let X be such a line, and let

$$(23) \quad x := X \cdot K, \quad x_i := X \cdot I, \quad x_j := X \cdot J.$$

Letting x', x'_i, x'_j be the images of these points under λ , we have

$$(24) \quad x' = \lambda(X) \cdot K', \quad x'_i = \lambda(X) \cdot I', \quad x'_j = \lambda(X) \cdot J'.$$

Since λ is a homology, then the lines $xx', x_i x'_i, x_j x'_j$ are concurrent at o , and so

$$(25) \quad (x'; x'_i, x'_j) = (x; x_i, x_j).$$

This gives

$$(26) \quad \frac{K'(\mu(x)) - I'(\mu(x))}{K'(\mu(x)) - J'(\mu(x))} = \frac{K(x) - I(x)}{K(x) - J(x)},$$

where x and $\mu(x)$ are the points obtained by projecting the lines X and $\lambda(X)$, respectively, from o_∞ to the real axis. Solving this for $\mu(x)$, one obtains (19). Now let

$$A(x) := \frac{K'(\mu(x)) - I'(\mu(x))}{K(x) - I(x)} = \frac{K'(\mu(x)) - J'(\mu(x))}{K(x) - J(x)}.$$

Then

$$K'(\mu(x)) - A(x)K(x) = I'(\mu(x)) - A(x)I(x) = J'(\mu(x)) - A(x)J(x).$$

Letting this quantity be $B(x)$, we obtain

$$K'(\mu(x)) = f(K(x)), \quad I'(\mu(x)) = f(I(x)), \quad J'(\mu(x)) = f(J(x)),$$

where

$$\begin{aligned} f(z) &= A(x)z + B(x) \\ &= \frac{K'(\mu(x)) - I'(\mu(x))}{K(x) - I(x)}z + \left[K'(\mu(x)) - \frac{K'(\mu(x)) - I'(\mu(x))}{K(x) - I(x)}K(x) \right] \\ &= \frac{K'(\mu(x)) - I'(\mu(x))}{K(x) - I(x)}z + \frac{K(x) \cdot I'(\mu(x)) - I(x) \cdot K'(\mu(x))}{K(x) - I(x)}. \end{aligned}$$

In other words, $\Omega \sim \Omega$ via the pair (μ, f) given by (19) and (20). The proof of theorem 4 is complete. \square

The homology λ is *harmonic* if, for any given point x , the harmonic conjugate of o with respect to x and its image x' lies on P , namely $xx' \cdot P$. For an explicit formula, we project from o_∞ the points $x, x', xx' \cdot P$, and o to the real axis $\mathbb{R} = (0, 1, 0)$, letting $x, \mu(x), p, q$ be the corresponding images. Since these points form a harmonic set, their cross-ratio is equal to -1 [10, page 38]:

$$(x, \mu(x); p, q) = \frac{(x; p, q)}{(\mu(x); p, q)} = -1,$$

from which we obtain

$$(27) \quad \mu(x) = \frac{Tx - 2D}{2x - T}, \quad \text{where} \quad T := p + q \quad \text{and} \quad D := pq,$$

which is indeed an involution since the associated matrix $\begin{pmatrix} T & -2D \\ 2 & -T \end{pmatrix}$ has zero trace [10, page 49].

Letting $o := (q, r)$, the aforementioned collinearity translates to

$$\det \begin{pmatrix} x & I'(x) & 1 \\ \mu(x) & I(\mu(x)) & 1 \\ q & r & 1 \end{pmatrix} = 0,$$

which determines the self-equivalence $I'(\mu(x)) = f(I(x))$, where

$$(28) \quad f(z) = \frac{\mu(x) - q}{x - q}z + \frac{x - \mu(x)}{x - q}r.$$

The same transformation applies to J and K .

A significant instance of this phenomenon occurs if the X-point is *regular*, for in this case λ exchanges I and J , since $I' = J$ and $J' = I$. If, in addition, the auxiliary function Y is regular, then o and Y are incident, so that formulae (27) and (28) apply with $r = Y(q)$.

Corollary 5. *If p is regular, then the homology λ is harmonic, and hence the associated function μ is an involution.*

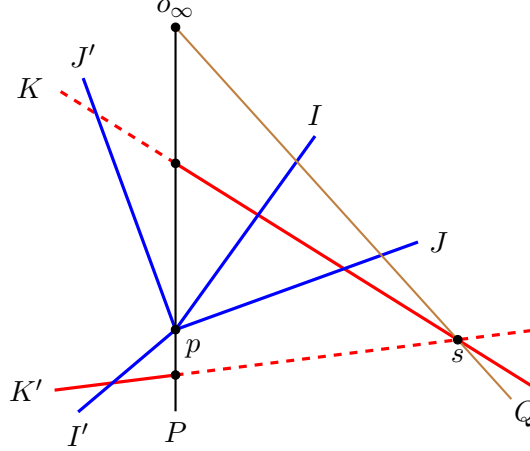


FIGURE 7. Construction of the projective collineation λ near a non-monotonic X-point p . The two branches K and K' of the auxiliary function of the pseudotriad do not meet on P .

3.2. Symmetry of pseudotriads. The triads considered so far will be relevant for X-points which are monotonic. The construction of an inheritable symmetry around a non-monotonic X-point —such as the point $p = \frac{1}{2}$ in the system $[0, x, 1]$ — requires a variant of the triad construct, a *pseudotriad*, characterised by the fact that the auxiliary function has two distinct components which do not meet on the line po_∞ . Specifically, one has

$$(29) \quad \Omega(x) = \begin{cases} [I, J; K](x) & \text{if } x \geq p \\ [I', J'; K'](x) & \text{if } x < p. \end{cases}$$

As before, I, J, I', J' are concurrent at p , and p is not on K or K' . If the median sequence is non-decreasing on the right of p and non-increasing on the left, then we have $J < I < K$ for $x > p$ and $K' < I' < J'$ for $x < p$. Otherwise, the primed and unprimed functions are exchanged. Our next result is the analogue of theorem 4 for non-monotonic X-points.

Theorem 6. *A pseudotriad (29) determines a projective collineation which maps the unprimed components to the corresponding primed ones and fixes o_∞ . Such a collineation, which is a homology if and only if the X-point is regular, induces a self-equivalence $\Omega \sim \Omega$ via the pair (μ, f) given by (19) and (20). This self-equivalence is unique up to inversion. The inverse of μ and the corresponding f are obtained by interchanging all primed and unprimed quantities.*

Proof. As for triads, the projective collineation λ is uniquely determined by the conditions (21). Since p is fixed, then the line $P := po_\infty$ is invariant under λ , but not pointwise; indeed $\lambda(K \cdot P) = K' \cdot P \neq K \cdot P$. First assume that the X-point is regular: $I = I'$ and $J = J'$. Then three lines through p are invariant, and hence all lines through p are invariant. Considering the invariant line ps , where $s := K \cdot K'$, we find that the point s is also fixed, and hence the line $Q := so_\infty$ is invariant. Now, at least one of the fixed points $I \cdot Q$ or $J \cdot Q$ is distinct from s (and obviously also from o_∞), and hence Q , having three fixed points, is pointwise invariant. Thus if p is regular, then λ is a homology with axis Q and centre p .

Now assume that p is not regular. Then the pencil through p has at most two fixed lines: P and P' (possibly with $P = P'$). Suppose for a contradiction that there exists a line L fixed by λ pointwise. If L does not contain p , then all lines through p are fixed, contradicting the fact that p is not regular. Otherwise, all lines through o_∞ are fixed, and so the two triples of points $o_\infty, I \cdot K, I' \cdot K'$ and $o_\infty, J \cdot K, J' \cdot K'$ are both collinear, which happens only if I' lie above J' on the affine plane, contradicting the fact that p is non-monotonic.

Thus, λ fixes no line pointwise, and hence is not a homology. Moreover, the pencil through o_∞ has at most two fixed lines: P and Q . Then $o := P' \cdot Q$ is the third fixed point of λ which, generically, is distinct from p and o_∞ . (The non-generic configurations which result in o coinciding with p or with o_∞ can be characterised using standard algebraic tools. We shall not pursue this matter here.)

To obtain the (μ, f) -self-equivalence, let X be a line through o_∞ , and let the points x, x_i , and x_j be given by (23). Moreover, let x', x'_i , and x'_j be their respective images under λ , i.e., (24). Since λ is projective, it preserves simple ratio, i.e., (25) holds. In other words, (26) holds, where x and $\mu(x)$ are the points obtained by projecting the lines X and $\lambda(X)$, respectively, from o_∞ to the real axis. Then one continues by repeating the same algebraic argument as in the proof of theorem 4, giving the desired self-equivalence. \square

An example is provided by the regular X-point $p = \frac{1}{2}$ in the system $[0, x, 1]$, where the median sequence is non-decreasing (non-increasing) on the right-hand (left-hand) side of p . The pseudotriad given by $I(x) = I'(x) = 3x - 1, J(x) = J'(x) = x, K(x) = 1, K'(x) = 0$, determines the homology with centre $(\frac{1}{2}, \frac{1}{2})$ and axis the line at infinity. The induced self-equivalence is given by $\mu(x) = 1 - x$ and $f(z) = 1 - z$, where μ is an involution. By contrast, the symmetry of the non-monotonic X-point $p = 0$ in the system $[-2, 0, x, 1]$ induces the Möbius transformation $\mu(x) = -2x$, which is not an involution.

4. THE SYSTEM $[0, x, 1, 1]$

In this section we shall describe a simple model for dynamics near an X-point which will be the basis for the theory for dynamics near a general X-point in the next section. The model is the initial bundle $[0, x, 1, 1]$, $x \in \mathbb{R}$, with its X-point $0 = Y_1 \bowtie Y_2$.

For this bundle, we will prove that the strong terminating conjecture holds globally (theorem 9) without using the computer algorithm of [2]. First, we show that the bundle possesses a global self-equivalence (lemma 7) which enables us to restrict our attention only to the right-hand side of the X-point. Next, we give an analytical description of its dynamics (figure 9) which exposes a dichotomy: at the X-point 0, the limit function has either a local minimum or a discontinuity (lemma 8). Finally, a computer is used to establish the first possibility by evaluating the limit function at a single judiciously chosen point.

To begin, let us write $\hat{\Xi}(x) := [0, x, 1, 1]$, where $x \in \mathbb{R}$. The bundle $\hat{\Xi}$ possesses the following global self-equivalence.

Lemma 7. *The self-equivalence $\hat{\Xi} \sim \hat{\Xi}$ holds globally via*

$$(30) \quad \mu(x) = \frac{x}{x-1} \quad \text{and} \quad f(z) = \frac{1}{1-x}z - \frac{x}{1-x}.$$

Proof. For every $x \in \mathbb{R}$, we have⁹

$$\begin{aligned} \left[0, \frac{x}{x-1}, 1, 1\right] &= \frac{1}{1-x} [0, -x, 1-x, 1-x] \\ &= \frac{1}{1-x} ([x, 0, 1, 1] - x) \\ &= \frac{1}{1-x} [0, x, 1, 1] - \frac{x}{1-x}, \end{aligned}$$

and hence the result. \square

We are now ready to prove that the strong terminating conjecture holds globally for $\hat{\Xi}$. The heart of our argument is the following lemma, which characterises the limit function of $\hat{\Xi}$ in the form of a dichotomy. The proof of this lemma is analytical, providing a complete description of the dynamics of $\hat{\Xi}$ near the X-point $0 = Y_1 \bowtie Y_2$ (figure 9). This proof will serve as the basis for the proof of the more general theorem 14 in the next section.

Lemma 8. *For the initial bundle $\hat{\Xi}$, exactly one of the following holds:*

i) *m is continuous at $x = 0$, and there exists $p_\infty \in (0, 1)$ such that*

$$m(x) = \begin{cases} \frac{1}{2p_\infty}x + \frac{1}{2} & \text{if } 0 \leq x < p_\infty \\ \frac{1}{2\mu(p_\infty)}x + \frac{1}{2} & \text{if } \mu(p_\infty) < x < 0 \\ 1 & \text{otherwise;} \end{cases}$$

ii) *m is discontinuous at $x = 0$ and*

$$m(x) = \begin{cases} \frac{1}{2} & \text{if } x = 0 \\ 1 & \text{otherwise.} \end{cases}$$

Proof. Let $\Xi_4 := \hat{\Xi}$. For every $n \geq 4$, let

$$Y_{n+1} := M(\Xi_n) \quad \text{and} \quad \Xi_{n+1} := \mathbf{M}(\Xi_n).$$

Moreover, for every $n \geq 4$, let

$$p_n := \max \{ \bar{p} \in \mathbb{Q} \cup \{\infty\} : \Xi_n \text{ is regular in } (0, \bar{p}) \}$$

and

$$q_n := \max \{ \bar{q} \in \mathbb{Q} \cup \{\infty\} : \Lambda_n \text{ is regular in } (0, \bar{q}) \},$$

where Λ_n denotes the core of Ξ_n , so that

$$U_n := (0, p_n) \quad \text{and} \quad V_n := (0, q_n)$$

are the domains of regularity of the bundle and the core, respectively, at time step n . In addition, let

$$I_n := \{x > 0 : Y_n(x) = 1\}, \quad \text{for every } n \geq 5,$$

and

$$H_n := \bigcup_{i=5}^n I_i, \quad \text{for every } n \geq 6.$$

Let us now study how U_n and V_n shrink as n increases. First, it is clear that $p_4 = \infty$ and $q_4 = 1$, and after direct calculation, $p_5 = 1$ and $q_5 = \frac{1}{3}$. In the next step, we take advantage

⁹We write $[a, b, c] \pm x$ to mean $[a \pm x, b \pm x, c \pm x]$.

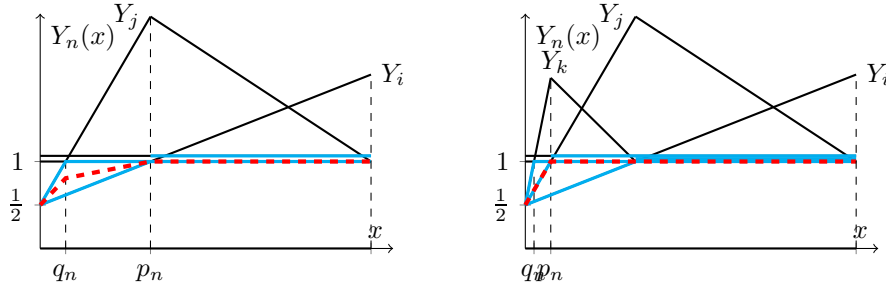


FIGURE 8. Even-to-odd iteration (left) and odd-to-even iteration (right).

of the fact that the rational set $\hat{\Xi}(0)$ stabilises immediately at $\frac{1}{2}$, which means that for every $n \geq 5$, the function Y_n passes through the point $o := (0, \frac{1}{2})$.

Now let $n \geq 5$. Our aim is to express p_{n+1} and q_{n+1} in terms of p_n and q_n . For this purpose, we shall focus our attention to the interval V_n and divide the analysis into two cases according to the parity of n :

CASE I: n is even. Let $\Lambda_n := [Y_i, Y_j]$, where $Y_i \leq Y_j$, as in Figure 8 (left). Then $Y_i(p_n) = Y_j(q_n) = 1$. Moreover, we have $\mathcal{M}_n = \langle Y_i, Y_j \rangle$ and $\mathcal{M}_{n-1} = Y_i$, and so by (11),

$$Y_{n+1} = \frac{n-1}{2} (Y_j - Y_i) + Y_j.$$

If $Y_i = Y_j$, then $Y_{n+1} = \mathcal{M}_n$, which means that the functional orbit *stabilises*, and

$$(31) \quad p_{n+1} = q_n \quad \text{and} \quad q_{n+1} = q_n.$$

If $Y_i < Y_j$, then Y_{n+1} is a new function lying above Y_j . Therefore,

$$(32) \quad p_{n+1} = q_n \quad \text{and} \quad q_{n+1} = \max(H_{n+1} \cap U_{n+1}).$$

CASE II: n is odd. Let $\Lambda_n = [Y_i, Y_j, Y_k]$, where $Y_i \leq Y_j \leq Y_k$, as in Figure 8 (right). Then $Y_j(p_n) = Y_k(q_n) = 1$. If $Y_j = Y_k$, then $\mathcal{M}_{n+1} = Y_j = \mathcal{M}_{n+2}$, so the functional orbit *stabilises*, and

$$(33) \quad p_{n+1} = q_n \quad \text{and} \quad q_{n+1} = q_n.$$

Now let $Y_j < Y_k$. Then $\mathcal{M}_n = Y_j$ and $\mathcal{M}_{n-1} = \langle Y_i, Y_j \rangle$, and so by (11),

$$Y_{n+1} = \frac{n}{2} (Y_j - Y_i) + Y_j.$$

If $Y_i = Y_j$, then $Y_{n+1} = \mathcal{M}_n$, which means that the functional orbit *stabilises*, and

$$(34) \quad p_{n+1} = p_n \quad \text{and} \quad q_{n+1} = p_n.$$

If $Y_i < Y_j$, then Y_{n+1} is a new function lying above Y_j . If $Y_{n+1} < Y_k$, then

$$(35) \quad p_{n+1} = p_n \quad \text{and} \quad q_{n+1} = \min I_{n+1}.$$

If $Y_{n+1} \geq Y_k$, then

$$(36) \quad p_{n+1} = p_n \quad \text{and} \quad q_{n+1} = q_n.$$

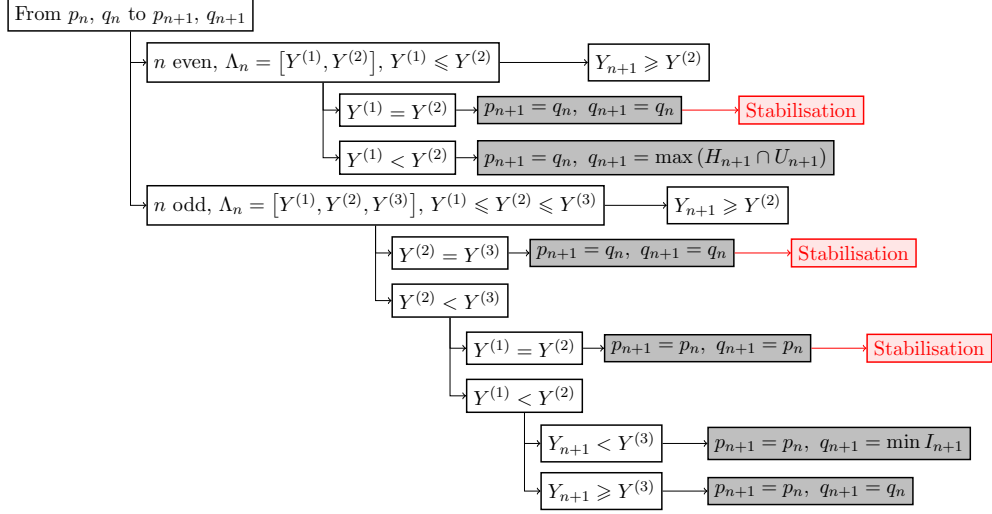


FIGURE 9. The flow chart for computing p_{n+1}, q_{n+1} from p_n, q_n .

Therefore, there are six different cases corresponding to six possible pairs of expressions of p_{n+1} and q_{n+1} in terms of p_n and q_n . These are summarised in figure 9.

We are now ready to determine the limit function of this bundle. By lemma 7, we have that $\hat{\Xi} \sim \hat{\Xi}$ via $\mu(x) = \frac{x}{x-1}$ and $f(z) = \frac{1}{1-x}z - \frac{x}{1-x}$. Here μ is an involution which maps the interval $(1, 2)$ to $(2, \infty)$ and the interval $(0, 1)$ to $(-\infty, 0)$. Taking advantage of the former, after straightforward computations we obtain that

$$(37) \quad m(x) = 1$$

and

$$\tau(x) = \begin{cases} 6 & \text{if } x \neq 2 \\ 5 & \text{if } x = 2 \end{cases}$$

for every $x \in [1, \infty)$.

Since we already know that $m(0) = \frac{1}{2}$ and $\tau(0) = 4$, it now remains to consider the case $x \in (0, 1)$. Notice that the sequence $(p_n)_{n=5}^{\infty}$ is non-increasing and bounded below by 0, and therefore it converges, say to $p_{\infty}^+ \in [0, 1)$. Moreover, every term of the sequence $(p_n)_{n=6}^{\infty}$ creates jump discontinuities of the transit time as described in lemma 3. Now there are two cases:

CASE I: $p_{\infty}^+ \in (0, 1)$. In this case the sequence $(p_n)_{n=5}^{\infty}$ either stabilises or converges without stabilising, and so the median sequence either stabilises at or converges without stabilising to

$$(38) \quad m(x) = \begin{cases} \frac{1}{2p_{\infty}^+}x + \frac{1}{2} & \text{if } 0 \leq x < p_{\infty}^+ \\ 1 & \text{if } x \geq p_{\infty}^+. \end{cases}$$

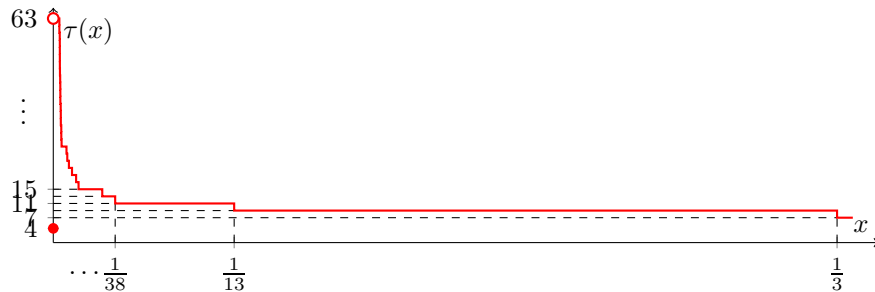


FIGURE 10. The transit time of $\hat{\Xi}$ for $x > 0$.

CASE II: $p_{\infty}^{+} = 0$. In this case the sequence $(p_n)_{n=5}^{\infty}$ converges without stabilising and the median sequence converges without stabilising to

$$(39) \quad m(x) = \begin{cases} 0 & \text{if } x = 0 \\ 1 & \text{if } x > 0. \end{cases}$$

Applying the self-equivalence to (38) and (39) gives the possible expressions of $m(x)$ for $x \in (-\infty, 0)$. Combining these with (37) gives the expressions in the lemma, thereby completing the proof. \square

Now, a single computer-aided evaluation of MMM orbit shows that, e.g., for $x_0 = 10^{-4}$, the set $\hat{\Xi}(x_0)$ stabilises at $m(x_0) = \frac{2597}{5000}$ with transit time $\tau(x_0) = 63$. Since the point $(x_0, m(x_0))$ is not on the auxiliary function, it follows that the first assertion of lemma 8 is true, and hence we have a bounded transit time as seen in figure 10. Moreover, by computing the abscissa of the point at which the line through o and $(x_0, m(x_0))$ intersects the auxiliary function, one obtains that $p_{\infty}^{+} = \frac{1}{388}$. Finally, we have that $p_{\infty}^{-} = \mu(p_{\infty}^{+}) = -\frac{1}{387}$, implying that the explicit formula of the limit function of this initial bundle is in fact as follows.

Theorem 9. *The strong terminating conjecture holds globally for the system $[0, x, 1, 1]$. Specifically, for every $x \in \mathbb{R}$ we have that $\tau(x) \leq 63$ and*

$$m(x) = Y_{63}(x) = \begin{cases} 1 & \text{if } x \leq -\frac{1}{387} \\ -\frac{387}{2}x + \frac{1}{2} & \text{if } -\frac{1}{387} < x < 0 \\ 194x + \frac{1}{2} & \text{if } 0 \leq x < \frac{1}{388} \\ 1 & \text{if } x \geq \frac{1}{388}. \end{cases}$$

5. DYNAMICS NEAR ACTIVE X-POINTS

We now turn to the analysis of the MMM dynamics near X-points. First, we develop suitable conditions under which the symmetry near a proper active X-point is inherited by the limit function (lemmas 10 and 11, theorem 13). Then we use our knowledge of the system $[0, x, 1, 1]$ to describe the limit function near any active X-point, dividing the analysis into two cases according to the rank of the X-point. Since the X-point 0 in the system $[0, x, 1, 1]$ is of rank 2, we first deal with general X-points of rank 2 or higher (theorem 14). Then we extend the

result to X-points of rank 1 (theorems 15 and 16). Finally, we justify the assumptions of our theorems by illustrating various pathologies.

In section 3, any function not through an X-point could be its auxiliary function. In this section, given an active X-point, we need to choose a specific auxiliary function which will be relevant to the future dynamics near the X-point. For this purpose, we define the *standard auxiliary function* and the *standard triad* of an active X-point $p = Y_i \bowtie Y_j$ —with a non-decreasing median sequence in its vicinity—to be $\min \mathcal{Y}_p$ and $[Y_i, Y_j; \min \mathcal{Y}_p]$, respectively, where \mathcal{Y}_p is defined by (14). Notice that the standard triad depends on Y_i and Y_j , whereas the standard auxiliary function does not; this is important if p is not proper.

5.1. Inheritance of symmetries and independence from previous history. In the bundle $\hat{\Xi}$, the standard triad of the proper active X-point 0 comprises the entire bundle (ignoring multiplicities), so it is obvious that the triad symmetry given by lemma 7 is inherited by the orbit of the bundle, leading to the functional equation (13). In general, however, we work with a triad which need not be the whole bundle, so whether the symmetry is inherited is not immediately apparent.

More precisely, consider a neighbourhood of an X-point p of a triad $\Omega = [Y_i, Y_j; Y]$ whose symmetry induces a self-equivalence via the pair (μ, f) . Our goal is to establish a sufficient condition under which (13) holds near p for the same pair (μ, f) . For this purpose, we will prove two lemmas. The first lemma characterises functions W which satisfy

$$(40) \quad W(\mu(x)) = f(W(x))$$

for the same pair (μ, f) . It turns out that these are precisely the *affine combinations*¹⁰ of functions in $\Omega^\downarrow := [Y_i \vee Y_j, Y_i \wedge Y_j, Y]$.

Lemma 10. *An affine function W which is regular except, possibly, at p , satisfies (40) if and only if W is an affine combination of functions in Ω^\downarrow .*

Proof. Write $U := Y_i \vee Y_j$, $L := Y_i \wedge Y_j$, and $f(z) = A(x)z + B(x)$ as in the proof of theorem 4. First suppose $W = \alpha U + \beta L + \gamma Y$, where $\alpha + \beta + \gamma = 1$. Then by theorem 4 we have

$$\begin{aligned} W(\mu(x)) &= \alpha U(\mu(x)) + \beta L(\mu(x)) + \gamma Y(\mu(x)) \\ &= \alpha f(U(x)) + \beta f(L(x)) + \gamma f(Y(x)) \\ &= \alpha[A(x)U(x) + B(x)] + \beta[A(x)L(x) + B(x)] + \gamma[A(x)Y(x) + B(x)] \\ &= A(x)[\alpha U(x) + \beta L(x) + \gamma Y(x)] + B(x)(\alpha + \beta + \gamma) \\ &= A(x)W(x) + B(x) \\ &= f(W(x)). \end{aligned}$$

Conversely, suppose that W is a piecewise-affine function with

$$(41) \quad W(\mu(x)) = f(W(x)) = A(x)W(x) + B(x)$$

for all x sufficiently close to p . We shall prove that W is an affine combination of U , L , and Y , i.e., that there exists $(\alpha, \beta) \in \mathbb{R}^2$ such that the functional identity

$$W = \alpha U + \beta L + (1 - \alpha - \beta)Y,$$

¹⁰Linear combinations with coefficients adding up to unity [8, page 428].

holds in a neighbourhood of p . This identity can be written as

$$\begin{cases} W(x) &= \alpha U(x) + \beta L(x) + (1 - \alpha - \beta)Y(x) \\ W(\mu(x)) &= \alpha U(\mu(x)) + \beta L(\mu(x)) + (1 - \alpha - \beta)Y(\mu(x)), \end{cases}$$

i.e.,

$$(42) \quad \begin{cases} Y(x) - W(x) &= [Y(x) - U(x)]\alpha + [Y(x) - L(x)]\beta \\ Y(\mu(x)) - W(\mu(x)) &= [Y(\mu(x)) - U(\mu(x))]\alpha \\ &+ [Y(\mu(x)) - L(\mu(x))]\beta. \end{cases}$$

But since near p we have

$$\begin{aligned} U(\mu(x)) &= A(x)U(x) + B(x), \\ L(\mu(x)) &= A(x)L(x) + B(x), \\ Y(\mu(x)) &= A(x)Y(x) + B(x), \end{aligned}$$

which, together with (41), imply

$$\begin{aligned} Y(\mu(x)) - W(\mu(x)) &= A(x)[Y(x) - W(x)], \\ Y(\mu(x)) - U(\mu(x)) &= A(x)[Y(x) - U(x)], \\ Y(\mu(x)) - L(\mu(x)) &= A(x)[Y(x) - L(x)], \end{aligned}$$

then the second equation in (42) is redundant (it is a multiple of the first equation), so it remains to show that the first equation has a solution $(\alpha, \beta) \in \mathbb{R}^2$. For this purpose, it suffices to show that $Y - U$ is not a multiple of $Y - L$. Suppose for a contradiction that there exists $k \in \mathbb{Q}$ such that $Y - U = k(Y - L)$. If $k = 1$, then $U = L$, which is a contradiction. Otherwise, we have

$$Y = \frac{1}{1-k}U - \frac{k}{1-k}L,$$

which means that the auxiliary function is an affine combination of the upper and lower concatenations of the X-point functions. This is also a contradiction because the auxiliary function does not pass through the X-point. \square

Now suppose the X-point $p = Y_i \bowtie Y_j$ is proper and active (the median sequence being non-decreasing in its vicinity), and the triad Ω is standard. We prove that, starting at the time step at which p stabilises, every function generated by the MMM is an affine combination of functions in Ω^\dagger , provided that the first one is. In this sense, the functional dynamics near p now depends only on functions in Ω^\dagger , rather than on all functions in its previous history.

Lemma 11. *Let p be a proper active X-point with standard triad Ω . If $Y_{\tau(p)}$ is an affine combination of functions in Ω^\dagger , then so is the function Y_n for every $n \geq \tau(p)$.*

Proof. Let p be a proper active X-point with standard triad Ω . Assume that $Y_{\tau(p)}$ is an affine combination of functions in Ω^\dagger . We use strong induction to prove that for every $n \geq \tau(p)$, the function Y_n is also an affine combination of functions in Ω^\dagger .

The base case is a part of the assumption. Now let $n \geq \tau(p)$ be such that every function in the set $[Y_{\tau(p)}, \dots, Y_n]$ is an affine combination of functions in Ω^\dagger . Then, from (11) we find that $Y_{n+1} = (n+1)\mathcal{M}_n - n\mathcal{M}_{n-1}$ is an affine combination of \mathcal{M}_n and \mathcal{M}_{n-1} , each of which is either a function in the set $[Y_{\tau(p)}, \dots, Y_n] \uplus \Omega^\dagger$ or the arithmetic mean of two such functions, and hence is an affine combination of functions in Ω^\dagger . This implies that Y_{n+1} is an affine combination of functions in Ω^\dagger , as easily verified. Therefore, the induction is complete. \square

Remark 12. Notice that lemma 11 remains true if Ω^\dagger is replaced by $\Omega^\dagger \setminus [Y]$, where Y is the standard auxiliary function of p , in which case $m(p) = Y_i(p) = Y_j(p)$. We will use this fact to prove proposition 17 in section 6.

From the above two lemmas, it is clear that if p is proper and active, and $Y_{\tau(p)}$ is an affine combination of functions in Ω^\dagger , where Ω is the standard triad of p , then all functions generated after its stabilisation satisfy the desired equivalence. Therefore we have achieved the goal of this section.

Theorem 13. Let p be a proper active X-point with standard triad Ω . If $Y_{\tau(p)}$ is an affine combination of functions in Ω^\dagger , then

$$(43) \quad Y_n(\mu(x)) = f(Y_n(x))$$

for every $n \geq \tau(p)$, and so (13) holds, and

$$(44) \quad \tau(\mu(x)) = \tau(x),$$

meaning that the functional orbit on the left-hand side stabilises if and only if that on the right-hand side stabilises.

We now understand why the structures of the limit function of the system $[0, x, 1]$ near every rational number in $[\frac{1}{2}, \frac{2}{3}]$ with denominator between 3 and 18 inclusive, as found in [2, theorem 1.3], are symmetric. As mentioned in section 2, these numbers are all X-points (figure 3) which are proper and active. Moreover, they possess local symmetries described by theorem 4 —as well as corollary 5 since they are regular— which are inherited to become local symmetries of the limit function.

5.2. The limit function near an X-point of high rank. In this subsection we generalise the dynamics near the X-point 0 of rank 2 in the bundle $\Xi(x) = [0, x, 1, 1]$ which was discussed in the proof of lemma 8. More precisely, we will prove a general version of lemma 8 which holds for active X-points of *high rank*, i.e., rank at least 2. To achieve this, we first need to identify a sufficient condition under which the dynamics near such an X-point is the exactly the same as the one described by figure 9, without any unwanted interaction with earlier functions, i.e., those appearing before the X-point stabilises. We will work only on the right-hand side of the X-point (therefore by *rank* we mean *right-rank*), where the median sequence is assumed to be non-decreasing, and define some terms which can be defined analogously on the left-hand side. In future discussions, the prefixes *right-* or *left-* may be added to each of these terms to avoid ambiguity. An active X-point p is said to be:

- *tractable* if there exists an odd integer $\ell \geq \tau(p)$ such that the following three conditions are satisfied:
 - T1** the median \mathcal{M}_ℓ meets the standard auxiliary function Y on the right-hand side of the X-point, say at $p_* \in (p, \infty)$, and both \mathcal{M}_ℓ and Y are regular in the interval $\mathcal{T} := (p, p_*)$;
 - T2** the interval \mathcal{T} contains no point $Y \bowtie \bar{Y}$, where $\bar{Y} \in \Xi_{\tau(p)-1}$;
 - T3** for every $n \in \{\tau(p), \dots, \ell\}$, the function Y_n has no corner below Y in \mathcal{T} .
 The smallest such number ℓ and the corresponding interval \mathcal{T} are referred to as the *tractability index* and *tractability domain* of the X-point, respectively.
- *dichotomic* in a neighbourhood¹¹ $[p, p_*)$ if the limit function $m : [p, p_*) \rightarrow \mathbb{R}$ is known to have exactly one of the following properties:

¹¹This neighbourhood may also be open, in which case the definition is modified by merely excluding p .

i) m is continuous at $x = p$, and in $[p, p_*)$ we have

$$(45) \quad m(x) = \begin{cases} \frac{Y(p_\infty) - m(p)}{p_\infty - p} x + \frac{p_\infty m(p) - p Y(p_\infty)}{p_\infty - p} & \text{if } p \leq x < p_\infty \\ Y(x) & \text{if } p_\infty \leq x < p_*, \end{cases}$$

for some $p_\infty \in (p, p_*)$.

ii) m is discontinuous at $x = p$, and in $[p, p_*)$ we have

$$(46) \quad m(x) = \begin{cases} m(p) & \text{if } x = p \\ Y(x) & \text{if } p < x < p_*. \end{cases}$$

We shall see that the tractability conditions **T1**, **T2**, and **T3** suffice to guarantee that a rescaled version of the dynamics described by figure 9 takes place on the right-hand side the active X-point, resulting in a dichotomy for the limit function as in lemma 8 in the tractability domain. More precisely, we shall prove the following theorem.

Theorem 14. *Any tractable X-point of rank at least 2 is dichotomic in its tractability domain.*

Proof. Let p be a tractable X-point of rank at least 2 with index ℓ , domain (p, p_*) , and standard auxiliary function Y . Then every median \mathcal{M}_k , $k \geq \tau(p) - 1$, and every function Y_k , $k \geq \tau(p)$, passes through the point $o := (p, m(p))$. For every $n \geq \ell$, let

$$p_n := \max \{ \bar{p} \in \mathbb{Q} : \text{all functions in } \Xi_n \text{ passing through } o \text{ and not below } \mathcal{M}_\ell \text{ are regular in } (p, \bar{p}) \},$$

and

$$q_n := \begin{cases} p_* & \text{if } n = \ell \\ \max \{ \bar{q} \in \mathbb{Q} : \Lambda_n \text{ is regular in } (p, \bar{q}) \} & \text{if } n \geq \ell + 1, \end{cases}$$

where Λ_n denotes the core of Ξ_n , so that

$$(47) \quad U_n := (p, p_n) \quad \text{and} \quad V_n := (p, q_n)$$

are the domain of regularity of the participating functions in the bundle and that of the core, respectively, at time step n . In addition, let

$$(48) \quad I_n := \{ x > p : Y_n(x) = Y(x) \}, \quad \text{for every } n \geq \tau(p),$$

and

$$(49) \quad H_n := \bigcup_{i=\tau(p)}^n I_i, \quad \text{for every } n \geq \ell + 1.$$

For every $n \geq \ell$, we express p_{n+1} and q_{n+1} in terms of p_n and q_n by dividing into cases in the same way as we have done for $\hat{\Xi}$, namely:

CASE I: n is even. Letting $\Lambda_n = [Y_i, Y_j]$, where $Y_i \leq Y_j$, we obtain

$$Y_{n+1} = \frac{n-1}{2} (Y_j - Y_i) + Y_j,$$

which implies (31) if $Y_i = Y_j$ or (32) if $Y_i < Y_j$.

CASE II: n is odd. Letting $\Lambda_n = [Y_i, Y_j, Y_k]$, where $Y_i \leq Y_j \leq Y_k$, we obtain

$$Y_{n+1} = \frac{n}{2} (Y_j - Y_i) + Y_j,$$

which implies (33) if $Y_j = Y_k$, (34) if $Y_i = Y_j$, (35) if $Y_i < Y_j$ and $Y_{n+1} < Y_k$, or (36) if $Y_i < Y_j$ and $Y_{n+1} \geq Y_k$.

This division into cases is once again summarised by figure 9, where the sets involved are those defined in (47), (48), and (49).

Since the sequence $(p_n)_{n=\ell}^\infty$ is non-increasing and bounded below by p , then it converges, say to $p_\infty \in [p, p_*]$. Moreover, every term of this sequence creates a jump discontinuity of the transit time as described in lemma 3. Now there are two cases. If $p_\infty > p$, then the sequence $(p_n)_{n=\ell}^\infty$ either stabilises or converges without stabilising, and so the median sequence either stabilises at or converges without stabilising to the function which emanates from o and meets Y at p_∞ , namely (45). If $p_\infty = p$, then the sequence $(p_n)_{n=\ell}^\infty$ converges without stabilising and the median sequence converges without stabilising to (46). The theorem is proved. \square

If an active X-point is dichotomic, a simple test adapted from the derivation of theorem 9 is applicable to ensure that the number p_∞ exists, i.e., that the first assertion for the limit function given in the dichotomy is true. Our next goal is to establish a result similar to theorem 14 for X-points of rank 1.

5.3. X-points of rank 1 and their auxiliary sequences. In the tractability domain of a tractable X-point of high rank, every subsequent function intersects the standard auxiliary function at a new regular X-point. Thus, the system generates a sequence of secondary X-points lying on the standard auxiliary function, which we shall call the *auxiliary sequence*. This sequence partitions the domain into adjacent subintervals, within which the dynamics has the simple structure prescribed by lemma 3, because the standard auxiliary function has high multiplicity.

If the X-point is of rank 1, then an auxiliary sequence of regular X-points is generated in exactly the same way. However, since the auxiliary function has unit multiplicity, between these secondary X-points the limit function no longer has a trivial form. In fact, as functions of high multiplicity are rare, each secondary X-point is typically of rank 1, and hence in turn possesses its own auxiliary sequence of tertiary X-points, each of which is typically of rank 1, and so on. There is, therefore, a hierarchical organisation¹² of X-points of rank 1.

To be more precise, we work on the right-hand side of an X-point p of (right-)rank 1 which is tractable with index ℓ and domain (p, p_*) , where the median sequence is assumed to be non-decreasing. Let $o := (p, m(p))$. The *auxiliary sequence* of p is the sequence $(p_n)_{n=\ell}^\infty$, where

$$p_n := \max \{ \bar{p} \in \mathbb{Q} : \text{all functions in } \Xi_n \text{ passing through } o \text{ and not below } \mathcal{M}_\ell \\ \text{are regular in } (p, \bar{p}) \},$$

for every $n \geq \ell$. Since p is tractable, the evolution of this sequence, together with that of its partner sequence $(q_n)_{n=\ell}^\infty$, where

$$q_n := \begin{cases} p_* & \text{if } n = \ell \\ \max \{ \bar{q} \in \mathbb{Q} \cup \{ \infty \} : \Lambda_n \text{ is regular in } (p, \bar{q}) \} & \text{if } n \geq \ell + 1, \end{cases}$$

for every $n \geq \ell$, is described in figure 9, where the sets involved are those defined in (47), (48), and (49). Therefore, we know the following properties of the auxiliary sequence.

¹²Thus, given a system, one would like to construct a tree which contains all its X-points and describes the hierarchy rigorously. This task is not easy and hence remains open.

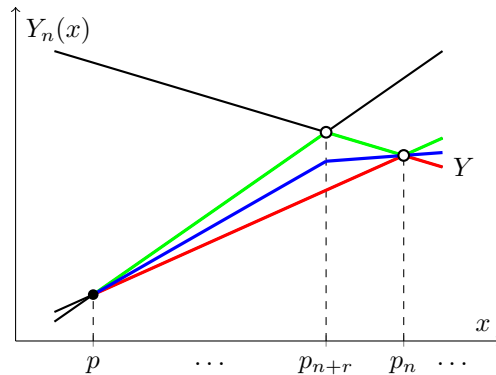


FIGURE 11. The medians $\mathcal{M}_{\tau(p_n)-2}$ (red), $\mathcal{M}_{\tau(p_n)-1}$ (blue), and $\mathcal{M}_{\tau(p_n)}$ (green), showing that $\tau(p_{n+r}) = \tau(p_n) + 2$.

Theorem 15. *The auxiliary sequence of a tractable X-point of rank 1 has the following properties:*

- i) *The sequence is non-increasing.*
- ii) *The sequence contains either infinitely or finitely many distinct regular X-points, each of which, except the last one in the latter case, is a local minimum of the limit function.*
- iii) *The transit times of the distinct terms of this sequence form an increasing arithmetic progression of common difference 2.*
- iv) *The sequence converges to p if and only if the limit function is discontinuous at p .*

Proof. Let p be an X-point of rank 1 which is tractable with index ℓ and standard auxiliary function Y . Part i) holds since the auxiliary sequence follows figure 9. We now prove parts ii) and iii).

Since the auxiliary sequence is non-increasing and bounded below by p , it converges. If it stabilises, it contains only finitely many distinct X-points. Otherwise, it contains infinitely many distinct X-points. Clearly, these X-points are all regular. Now let p_n be an arbitrary term of the auxiliary sequence which is not the term at which it stabilises. In its neighbourhood, the medians $\mathcal{M}_{\tau(p_n)-2}$ and $\mathcal{M}_{\tau(p_n)-1}$ are the lower concatenation and the average, respectively, of the two regular functions forming the X-point p_n . By lemma 1, it follows that $Y_{\tau(p_n)}$ lies above the upper concatenation of the X-point functions (except at p_n) which therefore becomes $\mathcal{M}_{\tau(p_n)}$. Since the limit function is at least the latter median, we have proved that p_n is a local minimum of the limit function.

Next, if r is the smallest positive integer for which $p_{n+r} < p_n$, then $\tau(p_{n+r}) = \tau(p_n) + 2$ (figure 11), and hence the transit times of the distinct terms of $(p_n)_{n=\ell}^{\infty}$ form an increasing arithmetic progression of common difference 2. The proof of parts ii) and iii) is complete.

Finally, suppose the auxiliary sequence converges to $p_{\infty} \in [p, p_{\ell}]$. If $p_{\infty} = p$, then the limit function is discontinuous at p . Otherwise, the limit function connects the points $(p, m(p))$ and $(p_{\infty}, Y(p_{\infty}))$, so it is continuous at p . We have therefore proved part iv). \square

Now suppose that the auxiliary sequence stabilises. In this case, the functional orbit near p stabilises and —assuming no unwanted interactions with earlier functions— its limit lies immediately above the second-to-last secondary X-point, making it an active high-rank X-point. By identifying its tractability domain, we can establish the shape of the limit function near p .

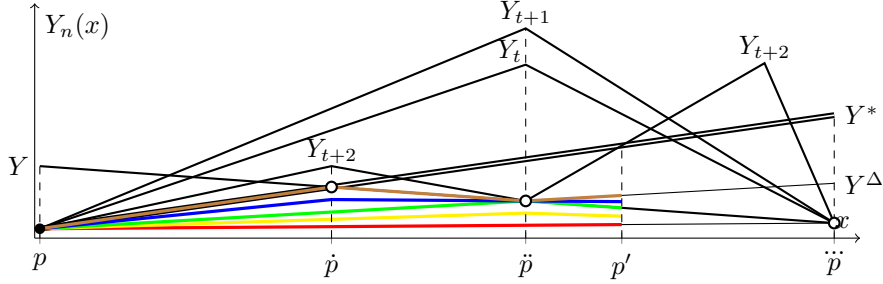


FIGURE 12. The situation in a right-neighbourhood of an X-point p of rank 1 if the functional orbit stabilises. Theorem 16 first describes, in part i), the limit function in $[p, \dot{p})$. If the extra condition in part ii) holds, then we can extend the description to $[p, p')$. The red, yellow, green, blue, and brown functions are the medians \mathcal{M}_{t-2} , \mathcal{M}_{t-1} , \mathcal{M}_t , \mathcal{M}_{t+1} , and \mathcal{M}_{t+2} , respectively.

Theorem 16. *Let p be a tractable X-point of rank 1 with standard auxiliary function Y and a stabilising auxiliary sequence, letting \ddot{p} , \dot{p} , and \check{p} be its last three distinct terms, assuming they exist. Suppose $\Xi_{\tau(p)-1}$ is regular in (p, \ddot{p}) and the number*

$$p' := \min \{x \in (\dot{p}, \ddot{p}) : Y_{\tau(\dot{p})}(x) = Y^*(x)\}$$

exists, where Y^ is the function at which the functional orbit near p stabilises.*

- i) *If for every $\bar{Y} \in \Xi_{\tau(p)-1} \setminus \{Y\}$ we have either $\bar{Y}(\dot{p}) < Y(\dot{p})$ or $\bar{Y}(p') > Y^*(p')$, then \dot{p} is a regular active X-point of high left-rank which is left-dichotomic in $[p, \dot{p})$ with Y^* as its standard auxiliary function.*
- ii) *If, in addition, in the interval (\dot{p}, \ddot{p}) we have that $p' < Y_{\tau(\dot{p})} \bowtie Y^*$, then \dot{p} is of high right-rank and is right-dichotomic in $[\dot{p}, p')$ with Y^* as its standard auxiliary function.*

Proof. Let p , \dot{p} , \ddot{p} , \check{p} , Y , and Y^* be as stated. Let $t := \tau(\ddot{p})$. Then, by part iii) of theorem 15, we have $\tau(\dot{p}) = t + 2$ and $\tau(\check{p}) = t + 4$. Let Y^Δ be the function in Ξ_{t-1} for which $\dot{p} = Y^\Delta \bowtie Y$.

Suppose the assumption of i) is true. Then it is clear that the X-point \dot{p} is regular, active, and has Y^* as its standard auxiliary function. Let us now prove that it has high left-rank. In the interval (p, \dot{p}) , the sequence $(\mathcal{M}_n)_{n=|\Xi|}^{t+2}$ is strictly increasing and $\mathcal{M}_{t+2} = \mathcal{M}_{t+3} = Y^*$, so Y^* belongs to Ξ_{t+2} with multiplicity at least two. Moreover, since $Y^* > Y^\Delta$ then $\mathcal{M}_{t+1} = \langle Y^*, Y^\Delta \rangle > Y^\Delta = \mathcal{M}_t$, so by lemma 1 we have $Y_{t+2} > Y^*$, in particular $Y_{t+2} \neq Y^*$, so $Y^* \in \Xi_{t+1}$ with multiplicity at least two. In other words, Ξ_{t+1} contains at least two functions \bar{Y} for which $\bar{Y}(x) = Y^*(x)$ for every $x \in (p, \dot{p})$. Since these functions are all regular in (p, \dot{p}) , then we have proved that \dot{p} has high left-rank. Moreover, the fact that \mathcal{M}_{t+2} meets Y^* at \dot{p} , together with the assumption, implies that \dot{p} is left-tractable with index $t + 2$ and domain (\dot{p}, \ddot{p}) , which means, by theorem 14, that \dot{p} is left-dichotomic in (\dot{p}, \ddot{p}) . But in $[p, \dot{p}]$ we have $m = Y^*$, so \dot{p} is left-dichotomic in $[p, \dot{p})$. Therefore we have proved i).

To prove ii), first notice that, in the open interval (p, \ddot{p}) , the functions Y_t and Y_{t+1} are singular only at \dot{p} where we have $Y_{t+1}(\dot{p}) > Y_t(\dot{p}) > Y^\Delta(\dot{p})$ by part i) of lemma 2 and lemma 1, knowing that $\mathcal{M}_{t-1}(\dot{p}) > \mathcal{M}_{t-2}(\dot{p})$. If the assumption holds, then—since the function Y_{t+2} is singular at \check{p} where $Y_{t+2}(\check{p}) > Y^*(\check{p})$ by lemma 1, at \dot{p} where $Y_{t+2}(\dot{p}) = m(p)$, and at another point on the right of p' — $Y_t(\check{p}) > Y^*(\check{p})$, so the situation is as in figure 12,

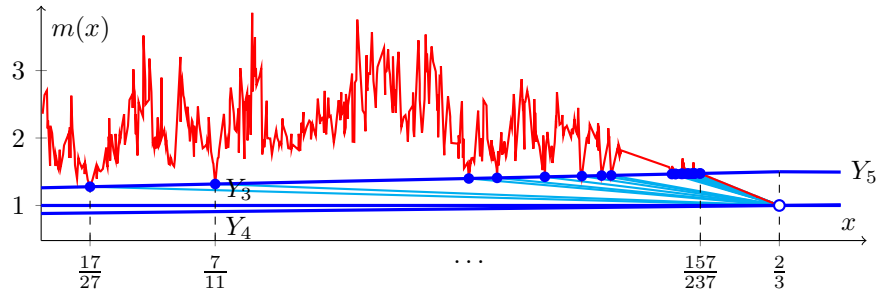


FIGURE 13. The situation in the left-tractability domain of the X-point $\frac{2}{3}$ of rank 1 in the system $[0, x, 1]$.

showing in particular that \ddot{p} has high right-rank, since in Ξ_{t+1} contains at least two functions \overline{Y} for which $\overline{Y}(x) = Y^*(x)$ for every $x \in (p, p')$. Since part i) of lemma 2 guarantees that $Y_{t+3}(p') > Y_{t+2}(p')$ and then lemma 1 guarantees that $Y_{t+4}(p') > Y_{t+2}(p')$, then \mathcal{M}_{t+4} meets Y^* at p' , so that \ddot{p} is right-tractable with index $t + 4$ and domain $[p, p']$. By theorem 14, it follows that \ddot{p} is right-dichotomic in $[p, p']$. \square

Let us apply theorems 15 and 16 on the left-hand side of the active X-point $\frac{2}{3} = Y_3 \bowtie Y_4$ of rank 1 in the system $[0, x, 1]$ which has limit 1 and transit time 7. This X-point is left-tractable with index 9 and domain $(\frac{17}{27}, \frac{2}{3})$. Figure 13 shows the left auxiliary sequence $(p_n)_{n=9}^\infty$ described by theorem 15 which stabilises and contains 27 distinct regular X-points, namely, $\frac{17}{27}, \frac{7}{11}, \dots, \frac{626}{945}, \frac{157}{237}$, in increasing order. By part ii) of the theorem, the first 26 X-points are local minima of the limit function lying on the standard auxiliary function Y_5 . Their transit times form an arithmetic sequence of difference 2, ranging from 11 to 63. Furthermore, the functional orbit stabilises at $Y^*(x) = -\frac{225}{2}x + 76$, and theorem 16 allows us to give a description of the limit function, firstly in $(\frac{626}{945}, \frac{2}{3}]$, in the form of a dichotomy, which is decidable by computing the orbit of a carefully chosen rational number near the X-point $\frac{626}{945}$ of rank 2. On the left-hand side of this X-point, we have a similar dichotomy for the limit function, decidable analogously. This gives the following formula of the limit function in the left neighbourhood $(\frac{12310}{18583}, \frac{2}{3}]$, which not only improves [2, equation (6)] but also uses significantly less computer assistance:

$$(50) \quad m(x) = \begin{cases} -\frac{225}{2}x + 76 & \text{if } \frac{12310}{18583} < x \leq \frac{50110610}{75646209} \\ -\frac{75675009}{256}x + \frac{25065033}{128} & \text{if } \frac{50110610}{75646209} \leq x < \frac{626}{945} \\ \frac{75647841}{256}x - \frac{25055657}{128} & \text{if } \frac{626}{945} \leq x < \frac{50130770}{75676641} \\ -\frac{225}{2}x + 76 & \text{if } \frac{50130770}{75676641} \leq x \leq \frac{2}{3}. \end{cases}$$

A similar analysis may be performed to improve the description of the limit function near every X-point of rank 1 in $[\frac{1}{2}, \frac{2}{3}]$ of denominator between 3 and 18 given in [2]. For instance, near $\frac{7}{12}$, theorem 16 gives eight (rather than two) branches of the limit function. In section 7 we will do the same for over 2000 X-points of rank 1 in the system.

5.4. Pathologies. We scrutinise the assumptions of the theorems in this section, describing various pathologies.

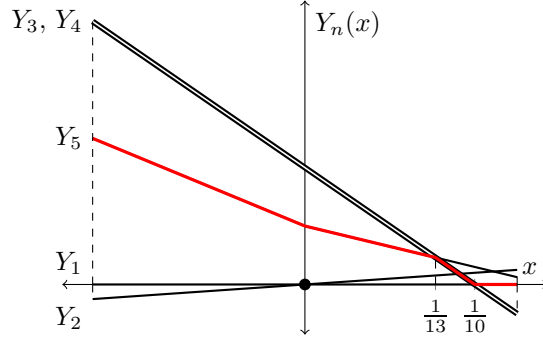


FIGURE 14. The first five functions in the system $[0, x, -10x + 1, -10x + 1]$ and their median (red).

i) *Standard triads whose symmetries are not inherited.* Consider the X-point $0 = Y_1 \bowtie Y_{n+1}$ in the system¹³

$$\hat{\Xi}^{(n)}(x) = \underbrace{[0, 0, \dots, 0]}_n, \underbrace{[x, 1, 1, \dots, 1]}_{n+1}, \quad \text{where } n \geq 2,$$

having limit $\frac{1}{2}$ and transit time $2n+3$. This X-point is regular, monotonic, active, of rank $n+1$, but not proper. Its standard triad $\Omega = [Y_1, Y_{n+1}; Y_{n+2}]$ is self-equivalent via (30). One checks that Y_{2n+3} is not self-equivalent via the same pair. However, the triad $\bar{\Omega} = [Y_{2n+3}, Y_{2n+4}; Y_{n+1}]$ associated to $0 = Y_{2n+3} \bowtie Y_{2n+4}$ is self-equivalent via

$$(51) \quad \mu(x) = \frac{nx}{x-1} \quad \text{and} \quad f(z) = \frac{1}{1-x}z - \frac{x}{1-x}.$$

Since $\mathcal{M}_{2n+3} = Y_{2n+3}$ and the median sequence is non-decreasing, then every function Y_k , $k \geq 2n+3$, is an affine combination of functions in $\bar{\Omega}^\dagger$, and so the self-equivalence via (51) is inherited and is satisfied by the limit function.

ii) *Non-tractability and different tractability indices on different sides of an X-point.* An X-point may be both left-tractable and right-tractable with different indices, or may be tractable only on one side. Indeed, consider the systems $[0, x, \alpha x + 1, \alpha x + 1]$, $\alpha \in \mathbb{Q}$, with X-point $0 = Y_1 \bowtie Y_2$ of rank 2, having limit $\frac{1}{2}$ and transit time 5.

For $\alpha = -10$, the function Y_5 intersects the standard auxiliary function at the point $(\frac{1}{13}, \frac{3}{13})$ only. Therefore, the median \mathcal{M}_5 meets the auxiliary function on the right-hand side of 0, namely at $\frac{1}{13}$, but not on the left-hand side (figure 14). Thus, the X-point is right-tractable with index $\ell = 5$. The next iteration gives the function

$$Y_6(x) = \begin{cases} \frac{3}{2}x + \frac{1}{2} & \text{if } x \geq 0 \\ -11x + \frac{1}{2} & \text{if } x < 0, \end{cases}$$

which intersects the auxiliary function at the points $(-\frac{1}{2}, 6)$ and $(\frac{1}{23}, \frac{13}{23})$. Since this function eventually becomes the median \mathcal{M}_7 , the X-point is left-tractable with index $\ell = 7$.

For $\alpha = -388$, the X-point is right-tractable but not left-tractable, because on the left-hand side of the X-point the median does not intersect the auxiliary function at all.

¹³For $n = 1$, this system is $[0, x, 1, 1]$, which is studied in section 4.

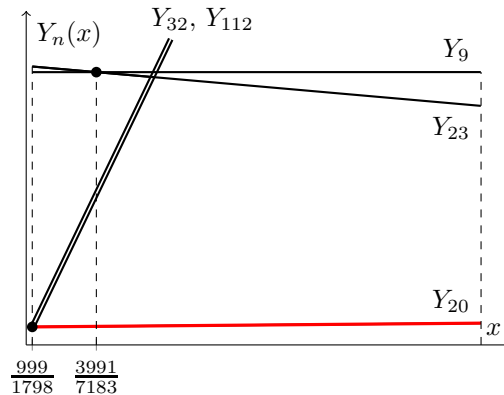


FIGURE 15. A violation of **T2** on the right-hand side of the X-point $\frac{999}{1798}$ in the system $[0, x, 1]$. The red function is the median \mathcal{M}_{25} .

iii) *Fulfilment of all but one tractability conditions.* For an active X-point p to be tractable, there must exist an odd time step $\ell \geq \tau(p)$ such that **T1**, **T2**, and **T3** are all satisfied. Let us now show that an odd time step $\ell \geq \tau(p)$ satisfying **T1** can either violate **T2** and satisfy **T3**, or violate **T3** and satisfy **T2**.

Consider the X-point $\frac{999}{1798} = Y_{12} \bowtie Y_{20}$ in the system $[0, x, 1]$, having limit $\frac{4685}{3596}$ and transit time 25. This X-point is regular, monotonic, proper, active, of rank 1, and its standard auxiliary function is $Y_9(x) = 15x - 7$. On the right-hand side of this X-point, the median \mathcal{M}_{25} intersects Y_9 at the point $(\frac{1867}{3360}, \frac{2267}{1699})$, and both \mathcal{M}_{25} and Y_9 are regular in the interval $\mathcal{T} = (\frac{999}{1798}, \frac{1867}{3360})$. Thus, the time step $\ell = 25$ satisfies **T1**. It also satisfies **T3**, since the function Y_{25} has no corner below Y_9 . However, $\frac{3991}{7183} = Y_9 \bowtie Y_{23} \in \mathcal{T}$, so ℓ does not satisfy **T2**. See figure 15.

Consider the X-point $0 = Y_4 \bowtie Y_5$ in the system $[-5, -4, -3, Y_4(x), x, 3, 3]$, where

$$(52) \quad Y_4(x) = \begin{cases} 0 & \text{if } x < \frac{1}{2} \\ x - \frac{1}{2} & \text{if } x \geq \frac{1}{2}, \end{cases}$$

having limit 0 and transit time 9. This X-point is regular, monotonic, proper, active, and of rank 2. Its standard auxiliary function is $Y_6(x) = 3$. On the right-hand side of this X-point, the median \mathcal{M}_9 intersects Y_6 at the point $(3, 3)$, and both \mathcal{M}_9 and Y_6 are regular in the interval $\mathcal{T} = (0, 3)$. Thus, the time step $\ell = 9$ satisfies **T1**. It also satisfies **T2**, since none of the functions Y_1, \dots, Y_8 intersect the auxiliary function at a point in \mathcal{T} . However, ℓ does not satisfy **T3**, since the function Y_9 has a corner $(\frac{1}{2}, \frac{11}{4})$, which lies below the auxiliary function Y_6 . See figure 16.

In section 7 we will describe further failures of tractability.

6. THE NORMAL FORM

In this section we will exploit further the fact that the functional dynamics near an X-point is eventually independent from most of its earlier history. We will construct the *normal form* of the MMM, which associates to every odd integer $t \geq 5$ an MMM-like dyadic rational sequence—called the *normal form orbit of order t*—which is equivalent to the functional MMM orbit

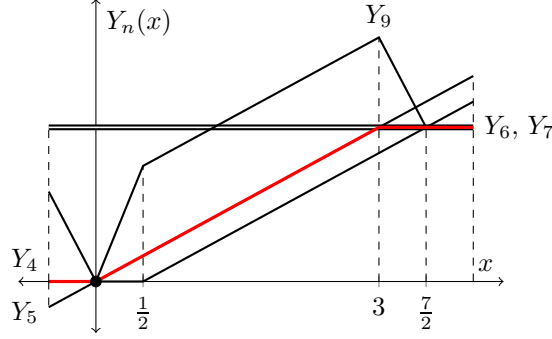


FIGURE 16. A violation of **T3** on the right-hand side of the X-point 0 in the system $[-5, -4, -3, Y_4(x), x, 3, 3]$, where Y_4 is defined in (52). The red function is the median \mathcal{M}_9 .

near any proper active X-point with transit time t in the system $[0, x, 1]$. Later, the number of such X-points is observed to grow exponentially with t (figure 19), so that verifying the stability of a single normal form orbit means verifying the strong terminating conjecture in the vicinity of exponentially many X-points.

Let us first discuss the construction of the normal form itself. Take an odd integer $t = 2h + 3 \geq 5$, and two sets $\xi^+ = [y_1^+, \dots, y_h^+]$ and $\xi^- = [y_1^-, \dots, y_h^-]$ of positive and negative numbers, respectively, satisfying

$$\sum_{i=1}^h y_i^+ + \sum_{i=1}^h y_i^- = -1.$$

For any $c \geq 1$, define the rational set

$$\xi := (\xi^- - c) \uplus [0, 1] \uplus (\xi^+ + c)$$

having even size $|\xi| = h + 2 + h = 2h + 2 = t - 1$, core $[0, 1]$, and median $\mathcal{M}_{t-1} = \mathcal{M}(\xi) = \frac{1}{2}$. One verifies that any set obtained from ξ by removing one element from $\xi^+ + c$ is an MMM preimage of ξ having median $\mathcal{M}_{t-2} = 0$.

Since the medians $\mathcal{M}_{t-2} = 0$ and $\mathcal{M}_{t-1} = \frac{1}{2}$ are both independent of c , the next iterate $y_t = t\mathcal{M}_{t-1} - (t-1)\mathcal{M}_{t-2}$ depends only on t , and not on c or ξ^\pm . Moreover, if c is sufficiently large, successive iterates will also depend only on t . Letting $c \rightarrow \infty$, we find that the whole sequence $(y_n)_{n=t}^\infty$ depends only on t —even if it is unbounded—and we call this sequence the *normal form orbit of order t* .

The *normal form* is thus a one-parameter family of dynamical systems, the parameter being an odd integer $t \geq 5$, which defines the initial data

$$\gamma_{t-1} := [0, 1], \quad \mathcal{M}_{t-2} := 0, \quad \mathcal{M}_{t-1} := \frac{1}{2}$$

and generates a sequence $(y_n)_{n=t}^\infty$, which depends only on t , via the recursion [cf. (11)]

$$(53) \quad y_n = n\mathcal{M}_{n-1} - (n-1)\mathcal{M}_{n-2} \quad \text{and} \quad \gamma_n = \gamma_{n-1} \uplus [y_n],$$

where $\mathcal{M}_n := \mathcal{M}(\gamma_n)$, for every $n \geq t$. Notice that all points in a normal form orbit are dyadic rational numbers, and the associated median sequence is non-decreasing. The significance of the normal form is given by the following proposition.

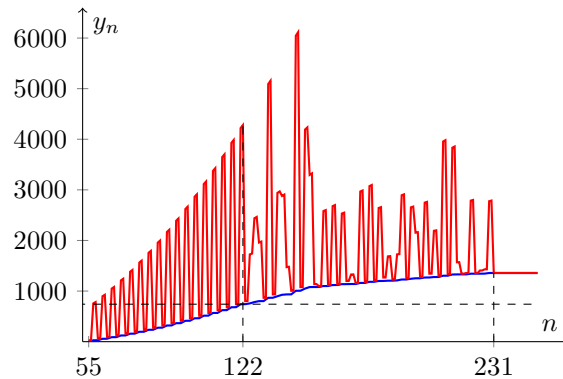


FIGURE 17. The normal form orbit of order 55 (red) and the corresponding median sequence (blue). The orbit behaves regularly up to $n = N_{55} = 122$, by lemma 18, which gives the explicit expressions for all terms up to this index. The horizontal dashed line represents the lower bound for the limit given by theorem 19, which is $740\frac{1}{2}$.

Proposition 17. *Let $p = Y_i \bowtie Y_j \in [\frac{1}{2}, \frac{2}{3}]$ be any proper active X-point in the system $\Xi_3(x) := [0, x, 1]$ with the property that $t := \tau(p) \geq 5$. On a side where $Y_i < Y_j$ we have*

$$(54) \quad Y_n(x) = [Y_j(x) - Y_i(x)] y_n + Y_i(x)$$

for every $n \geq t$. In particular, $(Y_n)_{n=t}^\infty$ stabilises if and only if $(y_n)_{n=t}^\infty$ stabilises.

Proof. Suppose the first sentence of the proposition holds. Consider a side of the X-point where $Y_i < Y_j$. Take an integer $n \geq t$. Near the X-point, $Y_t = t\mathcal{M}_{t-1} - (t-1)\mathcal{M}_{t-2} = t\langle Y_i, Y_j \rangle - (t-1)Y_i$ is an affine combination of elements of $[Y_i, Y_j]$, and hence by remark 12, so is Y_n . Similarly, in the normal form, y_t is an affine combination of elements of $[0, 1]$, and hence so is y_n . Now construct the unique affine transformation under which $0 \mapsto Y_i(x)$ and $1 \mapsto Y_j(x)$. This transformation is given by

$$z \mapsto [Y_j(x) - Y_i(x)] z + Y_i(x).$$

Since Y_n depends only on elements of $[Y_i, Y_j]$, y_n depends only on elements of $[0, 1]$, and the MMM preserves affine-equivalences, then we have $y_n \mapsto Y_n(x)$ under the same affine transformation. Therefore, we have the formula (54). \square

Therefore, the stabilisation of a normal form orbit implies the stabilisation of the functional orbits near all X-points having a particular transit time. We shall exploit this fact in section 7 to perform efficient computations. Meanwhile, let us conjecture that all normal form orbits stabilise.

Conjecture 4 (The strong terminating conjecture near proper active X-points). *For every odd integer $t \geq 5$, the normal form orbit of order t stabilises.*

Our next aim is to derive lower bounds for the limit m_t and the transit time τ_t of the normal form of order t . This will be achieved by establishing the existence of an initial phase of the orbit—the *regular phase*—whose length depends on t , and which admits an explicit description (figure 17).

For this purpose, we first note that the terms of the normal form orbit can also be generated by a recursion analogous to (8) which we shall now write down. Denote by λ_n the core of the set γ_n , for every $n \geq t - 1$. Then, for every $n \geq t + 1$, we have

$$(55) \quad y_n = \begin{cases} y_{n-1} + (y_j - y_i) & n \text{ even, } \lambda_{n-2} = [y_i, y_j] \\ y_{n-1} + \frac{n}{2}(y_k - y_j) - \frac{n-2}{2}(y_j - y_i) & n \text{ odd, } \lambda_{n-2} = [y_i, y_j, y_k], \end{cases}$$

where the core elements are written in non-decreasing order. We shall also use the increasing sequence $(u_\ell)_{\ell=0}^\infty$ with

$$u_\ell := \ell + 1 + \sqrt{5\ell^2 + 6\ell + 5}, \quad \text{for every } \ell \in \mathbb{N}_0.$$

The regular phase is described by the following lemma.

Lemma 18. *Let $t \geq 5$ be odd. Then*

$$y_t = \frac{t}{2}, \quad y_{t+1} = \frac{t}{2} + 1, \quad y_{t+2} = \frac{t^2}{4}, \quad y_{t+3} = \frac{t^2}{4} + \frac{t}{2} - 1,$$

with

$$(56) \quad 0 < 1 < y_t < y_{t+1} < y_{t+2} < y_{t+3}.$$

Moreover, for every $\ell \in \mathbb{N}$, if $t > u_\ell$ then

$$(57) \quad \begin{aligned} y_{t+4\ell} &= \frac{\ell+1}{2}t + \ell^2 + \ell, \\ y_{t+4\ell+1} &= \frac{\ell+1}{2}t + \ell^2 + \ell + 1, \\ y_{t+4\ell+2} &= \frac{t^2}{4} + \frac{5}{2}\ell t + 5\ell^2 - \ell, \\ y_{t+4\ell+3} &= \frac{t^2}{4} + \frac{5\ell+1}{2}t + 5\ell^2 + \ell - 1, \end{aligned}$$

with

$$(58) \quad y_{t+4\ell-3} < y_{t+4\ell} < y_{t+4\ell+1} < y_{t+2} \quad \text{and} \quad y_{t+4\ell-1} < y_{t+4\ell+2} < y_{t+4\ell+3}.$$

Proof. The proof involves straightforward applications of (55); we only outline the main steps. To prove the first assertion, we begin with $\gamma_{t-1} = [0, 1]$. Then (53) gives $y_t = \frac{t}{2}$ and $\gamma_t = [0, 1, \frac{t}{2}]$, and since $t \geq 5$, we find that $0 < 1 < y_t$. Next we compute y_{t+1} , y_{t+2} , y_{t+3} recursively, using (55); the condition $t \geq 5$ ensures that the chain of inequalities (56) is satisfied at each stage, as easily verified. This proves the first assertion.

The second assertion is proved by strong induction on $\ell \in \mathbb{N}$. The basis for induction is the statement that if $t \geq 7$ then

$$y_{t+4} = t + 2, \quad y_{t+5} = t + 3, \quad y_{t+6} = \frac{t^2}{4} + \frac{5}{2}t + 4, \quad y_{t+7} = \frac{t^2}{4} + 3t + 5,$$

with

$$(59) \quad y_{t+1} < y_{t+4} < y_{t+5} < y_{t+2} \quad \text{and} \quad y_{t+3} < y_{t+6} < y_{t+7}.$$

Starting with $\gamma_{t+3} = [0, 1, y_t, y_{t+1}, y_{t+2}, y_{t+3}]$ and the inequalities (56), we now apply (55) for $n \in \{t+4, t+5, t+6, t+7\}$. The condition $t \geq 7$ prescribes uniquely the position in the

sequence at which the numbers y_{t+4} and y_{t+5} must be inserted, as easily verified. We obtain the set γ_{t+7} whose terms satisfy the combination of (56) and (59), namely,

$$(60) \quad 0 < 1 < y_t < y_{t+1} < y_{t+4} < y_{t+5} < y_{t+2} < y_{t+3} < y_{t+6} < y_{t+7}.$$

The basis is proved.

Now suppose that the statements (57) and (58) hold for every $\ell \in \{1, 2, \dots, r-1\}$, for some $r \geq 2$. We prove that they also hold for $\ell = r$, assuming that $t > u_r$. Since $(u_\ell)_{\ell=0}^\infty$ is increasing, this implies that $t > u_\ell$ for every $\ell \in \{1, 2, \dots, r-1\}$, and hence our iteration proceeds up to and including the even-indexed term y_{t+4r-1} , while (60) extends to

$$(61) \quad \begin{aligned} 0 < 1 < y_t < y_{t+1} < y_{t+4} < y_{t+5} < \dots < y_{t+4r-4} < y_{t+4r-3} < y_{t+2} \\ < y_{t+3} < y_{t+6} < y_{t+7} < \dots < y_{t+4r-2} < y_{t+4r-1}. \end{aligned}$$

From the inductive hypothesis, we obtain the term

$$y_{t+4r-1} = \frac{t^2}{4} + \frac{5r-4}{2}t + 5r^2 - 9r + 3$$

as well as the odd core

$$\begin{aligned} \lambda_{t+4r-2} &= [y_{t+4r-7}, y_{t+4r-4}, y_{t+4r-3}] \\ &= \left[\frac{r-1}{2}t + r^2 - 3r + 3, \frac{r}{2}t + r^2 - r, \frac{r}{2}t + r^2 - r + 1 \right] \end{aligned}$$

which contains the three central elements in (61) before y_{t+4r-1} appears. Applying (55), we obtain

$$(62) \quad y_{t+4r} = \frac{r+1}{2}t + r^2 + r.$$

Using the above and the even core

$$\lambda_{t+4r-1} = [y_{t+4r-4}, y_{t+4r-3}] = \left[\frac{r}{2}t + r^2 - r, \frac{r}{2}t + r^2 - r + 1 \right]$$

which contains the two central elements in (61), a further application of (55) yields

$$(63) \quad y_{t+4r+1} = \frac{r+1}{2}t + r^2 + r + 1.$$

The elements (62) and (63) are now inserted into the chain of inequalities (61) at the positions uniquely determined by the assumption $t > u_r$. Finally, we apply (55) twice more, to obtain

$$y_{t+4r+2} = \frac{t^2}{4} + \frac{5}{2}rt + 5r^2 - r \quad \text{and} \quad y_{t+4r+3} = \frac{t^2}{4} + \frac{5r+1}{2}t + 5r^2 + r - 1$$

whose positions in the chain are again determined. Our set now is γ_{t+4r+3} with the corresponding chain of inequalities

$$(64) \quad \begin{aligned} 0 < 1 < y_t < y_{t+1} < y_{t+4} < y_{t+5} < \dots < y_{t+4r-4} < y_{t+4r-3} \\ < y_{t+4r} < y_{t+4r+1} < y_{t+2} < y_{t+3} < y_{t+6} < y_{t+7} < \dots \\ < y_{t+4r-2} < y_{t+4r-1} < y_{t+4r+2} < y_{t+4r+3}. \end{aligned}$$

which agrees with (58) for $\ell = r$. The lemma is proved. \square

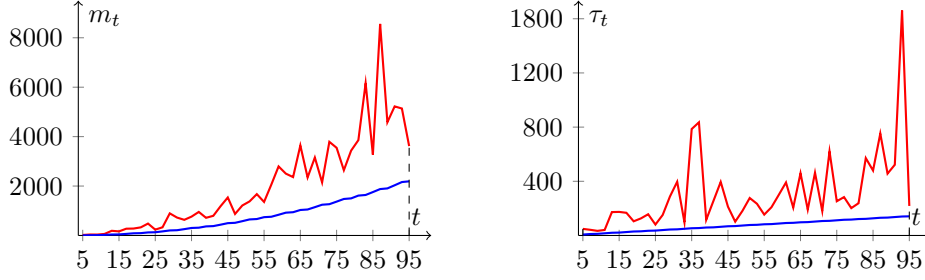


FIGURE 18. Plots of m_t (left) and τ_t (right) for $t \in \{5, 7, \dots, 95\}$ with the respective lower bounds given by theorem 19.

Lemma 18 gives the explicit formula of every term of the orbit up to that of even index

$$N_t := t + 4L_t + 3,$$

where

$$L_t := \max \{ \ell \in \mathbb{N}_0 : t > u_\ell \} = \left\lceil \frac{-t - 2 + \sqrt{5t^2 - 4t - 12}}{4} \right\rceil - 1,$$

along with the associated chain of inequalities. These terms are all distinct because each inequality is strict. Since the next two terms y_{N_t+1} and y_{N_t+2} also obey the formulas given in lemma 18, we find that for every odd integer $t \geq 5$,

$$(65) \quad y_{N_t+1} = \frac{L_t + 2}{2}t + L_t^2 + 3L_t + 2 \quad \text{and} \quad y_{N_t+2} = \frac{L_t + 2}{2}t + L_t^2 + 3L_t + 3.$$

Although certainly $y_{N_t+1} < y_{N_t+2}$, we do not make any statement regarding the positions of these two terms in the chain of inequalities, which may depend on t .

Since stabilisation has not occurred at time step $N_t + 2$, we have established a lower bound for the transit time τ_t . From (64) we know that $\lambda_{N_t} = [y_{t+4L_t}, y_{t+4L_t+1}]$, and hence $m_t \geq y_{t+4L_t+1}$, since the median sequence is non-decreasing. We have established the following bounds:

Theorem 19. *For every odd $t \geq 5$ we have*

$$\begin{aligned} m_t &\geq \frac{L_t + 1}{2}t + L_t^2 + L_t + 1 \sim \frac{t^2}{4} \\ \tau_t &\geq N_t + 2 \sim t\sqrt{5}. \end{aligned}$$

The plots of m_t and τ_t for $t \in \{5, 7, \dots, 95\}$ with the respective lower bounds are shown in figure 18. All available evidence suggests that, for sufficiently large t the limit m_t is also bounded above by the value of the largest term in the regular phase.

Conjecture 5. *For every odd integer $t \geq 9$, we have $m_t < y_{N_t}$.*

We conclude this section with some remarks on the arithmetic of normal form orbits. Given an odd integer $t \geq 5$, we are interested in the smallest ring $\mathbb{K} \subset \mathbb{R}$ which contains the whole normal form orbit of order t . Because (53) only produces rational numbers whose denominators are powers of 2, it is clear that $\mathbb{K} \subset \mathbb{Z}[\frac{1}{2}]$ (the set of rationals whose denominator is a power of 2). With this in mind, we recall that the *2-adic valuation* $\nu_2 : \mathbb{N} \rightarrow \mathbb{N}_0$ is given by [5, page 562]

$$\nu_2(b) := \max \{ i \in \mathbb{N}_0 : 2^i \mid b \}$$

for every $b \in \mathbb{N}$.

For every $n \geq t$, we define the n -th effective exponent¹⁴ as the maximum 2-adic value of the denominators of the iterates y_t, \dots, y_n in lowest terms, so that

$$\gamma_n \subset \frac{1}{2^{\kappa(n)}}\mathbb{Z}.$$

The 2-adic value of the denominator of the median \mathcal{M}_n is at most $\kappa(n)$ if n is odd and at most $\kappa(n) + 1$ if n is even. Since $\kappa(t) = \kappa(t + 1) = 1$, an easy induction shows that for every $n \geq t$ we have [6, proposition 2.5]

$$\kappa(n) \leq \left\lfloor \frac{n - t + 2}{2} \right\rfloor.$$

The above bound is very crude. Due to sustained cancellations, the actual exponent is much smaller, but its determination seems problematic. However, an exact expression for the effective exponent is available during the regular phase of the orbits. Since t is odd, we can see in lemma 18 and equation (65) that the 2-adic value of the denominator of each number in γ_{N_t+2} is the maximum of the 2-adic values of the denominators of the coefficients in its explicit formula. Since these denominators are at most 4, we have:

Corollary 20. *For every odd integer $t \geq 7$, we have $\kappa(N_t + 2) = 2$.*

7. COMPUTATIONS

We conclude by presenting an account of our computations of the limit function. The existing results are those in [2], where the strong terminating conjecture for $[0, x, 1]$ was established in neighbourhoods of all 18 rational numbers with denominator at most 18 lying in the interval $I := [\frac{1}{2}, \frac{2}{3}]$. In these neighbourhoods, whose measure adds up to 11.75% of the total, the limit function is piecewise-affine with finitely many pieces and 26 corners.

We have extended these computations considerably, determining neighbourhoods of quasi-regularity around over 2000 rational points and generating a sequence of lower bounds for the total variation of the limit function. Conjecture 3, stated at the end of the introduction, represents a synthesis of our findings, which we now describe in some detail.

7.1. Neighbourhoods of quasi-regularity. By computing the orbit using exact rational arithmetic, we have established that the normal form orbit of order t stabilises for $t \in \{5, \dots, 999\}$. This means that every proper active X-point p with $\tau(p) \leq 1000$ has a neighbourhood in which the strong terminating conjecture holds.

This computation, however, does not yield an estimate of the size of these neighbourhoods. We have implemented a procedure which associates to every X-point p a neighbourhood U_p in which the strong terminating conjecture holds, which we call the *neighbourhood of quasi-regularity* of p . Achieving optimal convergence for the total measure of the U_p s requires ordering the X-points p by the decreasing size of U_p . However, this ordering is not available; indeed $|U_p|$ has only a tenuous connection with the *height*¹⁵ of p and with the transit time $\tau(p)$. We have therefore adopted a hybrid approach.

I: ORDERING BY TRANSIT TIME. We have constructed the set

$$\mathcal{X}_t = \{p \in I : p \text{ is an X-point with } \tau(p) = t\}.$$

¹⁴Notice that the sequence $(\kappa(n))_{n=t}^{\infty}$ is non-decreasing.

¹⁵The maximum of the absolute value of the numerator and denominator.

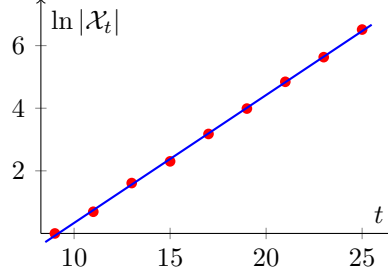


FIGURE 19. Least-square regression plot associated to (66).

for every odd integer t with $5 \leq t \leq 25$, by computing explicitly the bundle Ξ_{23} and identifying all its active X-points. Some of the data are

$$\mathcal{X}_9 = \left\{ \frac{7}{12} \right\}, \quad \mathcal{X}_{11} = \left\{ \frac{9}{16}, \frac{17}{27} \right\}, \quad \text{and} \quad \mathcal{X}_{13} = \left\{ \frac{29}{54}, \frac{67}{116}, \frac{45}{76}, \frac{19}{31}, \frac{7}{11} \right\}.$$

The set $\mathcal{X} = \bigcup_{\substack{9 \leq t \leq 25 \\ t \text{ odd}}} \mathcal{X}_t$ has 1176 elements, all of which are X-points of rank 1. The data

t	9	11	13	15	17	19	21	23	25
$ \mathcal{X}_t $	1	2	5	10	24	54	127	279	674

suggest that $|\mathcal{X}_t|$ grows exponentially with t (figure 19):

$$(66) \quad |\mathcal{X}_t| \approx 0.024e^{0.41t}.$$

Given p , we specify U_p as follows. After generating the required data associated to p , we check the validity of the following conditions on the right-hand side of p , as well as analogous conditions on the left-hand side (notation as in theorem 16 and figure 12).

- i) For every distinct $\bar{Y}, \bar{\bar{Y}} \in \Xi_{\tau(p)-1}$ we have $\bar{Y} \bowtie \bar{\bar{Y}} \notin (p, \ddot{p})$.
- ii) For every $\bar{Y} \in \Xi_{\tau(p)-1} \setminus [Y]$ we have either $\bar{Y}(\ddot{p}) < Y(\ddot{p})$ or $\bar{Y}(p') > Y^*(p')$.
- iii) In $(\ddot{p}, \ddot{\bar{p}})$ we have $p' < Y_{\tau(\ddot{p})} \bowtie Y^*$.

Out of all 1176 X-points, 1092 satisfy all three conditions on both sides, and for these points theorem 16 applies to both sides. For such X-points p , we let U_p be the neighbourhood given by the theorem.

Of the remaining 84 X-points, 52 only violate iii), but on both sides. On each side, theorem 16 enables us to conclude that the strong terminating conjecture holds up to the second-to-last term of the auxiliary sequence. Therefore, U_p can also be specified without difficulty.

None of the remaining 32 X-points violate ii); they violate either i) only, or both i) and iii), on at least one side. On the right-hand side, if i) is violated, then regardless of whether iii) is violated, theorem 16 does not apply. However, we know that the strong terminating conjecture holds in the interval (p, \bar{p}) , where

$$\bar{p} := \min \left\{ \bar{Y} \bowtie \bar{\bar{Y}} \in (p, \ddot{p}) : \bar{Y}, \bar{\bar{Y}} \in \Xi_{\tau(p)-1} \right\}.$$

Treating the left-hand side similarly, we obtain U_p .

The total measure $\sum_{p \in \mathcal{X}} |U_p|$ of these neighbourhoods of quasi-regularity amounts to 3.12% of the length of I . Combining this with the result near $\frac{1}{2}$ obtained in [2], which covers 7.29%, and the result near $\frac{2}{3}$ in (50), which covers 2.54%, we conclude that the strong terminating

conjecture holds over 12.95% of the domain I . These neighbourhoods of 1178 rational numbers contain 7918 corners of the limit function.

II: ORDERING BY HEIGHT. An exhaustive search of X-points with larger transit time is not feasible. Considering that some rationals in \mathcal{X} have a very large height (the largest being 571460), we have supplemented the above data with a selected collection of X-points of higher transit time, having moderate height. Specifically, we have considered the set

$$\{p \in \mathcal{F}_{5000} \cap I : p \text{ is an X-point with } \tau(p) \in \{27, 29, 31\}\},$$

where \mathcal{F}_{5000} is the set of all fractions with denominator at most 5000. This set contains 1618 active X-points, all of rank 1. Of those, 1616 satisfy all three conditions i), ii), iii) on both sides, and hence theorem 16 applies, and we let U_p be the neighbourhood given by the theorem. It is worth mentioning that 3 of these 1616 points are not proper. Each of these X-points is a transversal intersection of three distinct functions appearing before the X-point stabilises, and has neither an inherited symmetry nor a connection to the normal form. The local stabilisation is thus verified by evaluating MMM orbits at suitable points (cf. establishment of theorem 9 in the paragraph preceding it). The remaining two X-points are:

- $p = \frac{708}{1273}$ with $\tau(p) = 29$, which violates iii) on the right-hand side; theorem 16 only enables us to conclude that the strong terminating conjecture holds up to the second-to-last term \check{p} of the auxiliary sequence; so the right part of U_p is replaced by $(p, \frac{722540}{1299143})$.
- $p = \frac{1913}{3452}$ with $\tau(p) = 27$, which violates ii) on the right-hand side; the function Y_{25} intersects the limit function at $\frac{20613}{37196}$, and so the right part of U_p is replaced by $(p, \frac{20613}{37196})$.

This additional computation adds 1618 to the number of X-points, 11321 to the number of corners of the limit function, but only 0.21% to the total measure. In conclusion, we have proved that the strong terminating conjecture holds for $[0, x, 1]$ in specified neighbourhoods of 2794 X-points which cover 13.16% of the domain I and contain 19239 corners of the limit function.

From this result, it seems plain that the neighbourhoods of quasi-regularity associated with the X-points do not account for the full measure. At the same time, the available evidence strongly suggests that these neighbourhoods form a *dense* subset of I .

7.2. Total variation of limit function and box dimension of its graph. To gain insight on the region outside the neighbourhoods of quasi-regularity, we turn our attention to the *total variation* [9, section 6.3] of the limit function. We have computed the variation $V(q)$ of the limit function with respect to the Farey partition $\mathcal{F}_q \cap I$ —the set of fractions with denominator up to q in I —for $q \in \{3, \dots, 2000\}$, with the finest partition containing 202,768 points. The data show a steady algebraic growth of $V(q)$, with exponent $\alpha \approx 0.86$ (figure 20).

The Farey partition is only approximately uniform. For additional evidence, and to afford a dimension estimate, we have computed the variation of the limit function with respect to the partition $\frac{1}{2^i}\mathbb{Z} \cap I$ for $i \in \{3, \dots, 14\}$. Consistently, the data show an algebraic growth with a similar exponent $\alpha \approx 0.85$.

To connect variation to dimension, let us consider a uniform partition of I into $n \in \mathbb{N}$ intervals of length $\epsilon_n := \frac{1}{6n}$, namely $\{x_i\}_{i=0}^n$ with $x_i := \frac{1}{2} + i\epsilon_n$ for every $i \in \{0, \dots, n\}$. Letting $V'(n)$ be the variation of the limit function with respect to this partition, we find

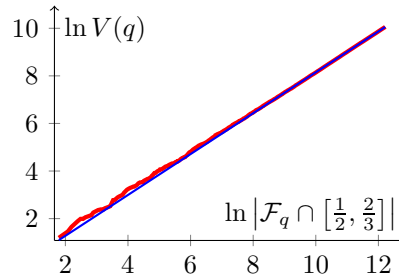


FIGURE 20. Log-log plot of the variation of the limit function with respect to the Farey partition versus the size of the partition. The slope of the line is approximately 0.86.

that

$$\frac{V'(n)}{\epsilon_n} = \sum_{i=1}^n \frac{|m(x_i) - m(x_{i-1})|}{\epsilon_n} \xrightarrow{n \rightarrow \infty} N(\epsilon_n),$$

where $N(\epsilon_n)$ denotes the minimum number of ϵ_n -boxes needed to cover the graph

$$\mathcal{G} := \{(x, m(x)) : x \in I\},$$

assuming continuity. Consequently, if $V'(n) \sim cn^\alpha$ for some $c, \alpha > 0$, then the box dimension of \mathcal{G} is given by

$$\dim_B(\mathcal{G}) = \lim_{n \rightarrow \infty} \frac{\ln N(\epsilon_n)}{-\ln \epsilon_n} = \lim_{n \rightarrow \infty} \frac{\ln \frac{V'(n)}{\epsilon_n}}{-\ln \epsilon_n} = 1 + \lim_{n \rightarrow \infty} \frac{\ln cn^\alpha}{\ln 6n} = 1 + \alpha.$$

We believe that the fractional dimension of the limit function originates entirely from the region outside the neighbourhoods of quasi-regularity. Indeed, the portion of \mathcal{G} corresponding to the neighbourhoods of quasi-regularity can be modelled as a family of non-overlapping V-shapes, constructed recursively in such a way that their number grows exponentially, while their width decreases exponentially. Regardless of the growth of the height of these V-shapes, one finds that the resulting set has box dimension one. This motivates our conjecture 3.

Finally, we have detected no evidence of multifractal behaviour. Our computation of the variation of the limit function in a few smaller subintervals has given algebraic growth with similar exponents.

ACKNOWLEDGEMENTS: The first author thanks Indonesia Endowment Fund for Education (LPDP) for the financial support.

REFERENCES

- [1] P. C. Allaart and K. Kawamura, The Takagi function: a survey, *Real Analysis Exchange*, **37** (2011), 1–54.
- [2] F. Cellarosi and S. Munday, On two conjectures for M&m sequences, *Journal of Difference Equations and Applications*, **22** (2016), 428–440.
- [3] M. Chamberland and M. Martelli, The mean-median map, *Journal of Difference Equations and Applications*, **13** (2007), 577–583.
- [4] H. S. M. Coxeter, *Projective Geometry*, Springer, New York, 1987.
- [5] G. H. Hardy and E. M. Wright, *An Introduction to the Theory of Numbers*, 6th edition, Oxford University Press, Oxford, 2008.
- [6] J. Hoseana, *The Mean-Median Map*, MSc dissertation, Queen Mary University of London, 2015.

- [7] J. C. Lagarias, The Takagi function and its properties, in *Functions in Number Theory and their Probabilistic Aspects* (eds. K. Matsumoto, Editor in Chief, S. Akiyama, H. Nakada, H. Sugita, A. Tamagawa), RIMS Kôkyûroku Bessatsu B34, (2012), 153–189.
- [8] S. Roman, *Advanced Linear Algebra*, 3rd edition, Springer, California, 2007.
- [9] H. L. Royden and P. M. Fitzpatrick, *Real Analysis*, 4th edition, Prentice Hall, Boston, 2010.
- [10] H. Schwerdtfeger, *Geometry of Complex Numbers*, Dover, New York, 1979.
- [11] H. Schultz and R. Shiflett, M&m sequences, *College Mathematics Journal*, **36** (2005), 191–198.

SCHOOL OF MATHEMATICAL SCIENCES, QUEEN MARY, UNIVERSITY OF LONDON, LONDON E1 4NS, UK